Molecular Pharmacology Fast Forward. Published on August 29, 2016 as DOI: 10.1124/mol.116.105361
This article has not been copyedited and formatted. The final version may differ from this version.

MOL #105361

An Aryl Hydrocarbon Receptor-mediated Amplification Loop that Enforces Cell Migration in ER$^-$/PR$^-$/Her2$^-$ Human Breast Cancer Cells

Olga Novikov, Zhongyan Wang , Elizabeth A. Stanford, Ashley J. Parks, Alejandra Ramirez-Cardenas, Esther Landesman, Israa Laklouk, Carmen Sarita-Reyes, Daniel Gusenleitner, Amy Li, Stefano Monti, Sara Manteiga, Kyongbum Lee and David H. Sherr

Boston University School of Public Health, Department of Environmental Health, 72 E. Concord Street, Boston, MA 02118 (ON, ZW, EAS, AJLP, AR-C, DHS)

Boston University Molecular and Translational Medicine Program, 72 E. Concord Street, Boston MA 02118 (ON, EAS)

Boston University School of Medicine, Department of Medicine, Division of Computational Biomedicine, Boston, MA 02118 (DG, AL, SMo)

Boston University School, Department of Pathology and Laboratory Medicine (EL, CS-R, IL)

Tufts University, Department of Chemical and Biological Engineering, Medford, MA, 02155 (SMa, KL)

Molecular Pharmacology Fast Forward. Published on August 29, 2016 as DOI: 10.1124/mol.116.105361
This article has not been copyedited and formatted. The final version may differ from this version.

MOL #105361

Running Title: An AHR/TDO amplification loop drives breast cancer cell migration

Corresponding author: David H. Sherr, Ph.D., Department of Environmental Health, Boston University School of Public Health, 72 East Concord Street (R-408), Boston, Massachusetts, 02118. Phone: 617-638-6464, FAX: 617-638-6463, dsherr@bu.edu

Text pages: 17

Tables: 0

Figures: 12

References: 149

Abstract: 248 words

Introduction: 743 words

Discussion: 1364 words

Abbreviations

AHR, Aryl hydrocarbon receptor; B[a]P, benzo[a]pyrene; bHLH/PAS, Helix-Loop-Helix/Per-Arnt-Sim; CCLE, Cancer Cell Line Encyclopedia; DMSO, dimethyl sulfoxide; DNA, deoxyribonucleic acid; DOX, doxycycline; $ER^-/PR^-/Her2^-$, Estrogen, Progesterone, Human epidermal growth factor 2 receptor negative; FICZ, 6-Formylindolo[3,2-b]carbazole; IBC; inflammatory breast cancer; IDO1/2, Indolamine-2,3-dioxygenase 1/ Indolamine-2,3-dioxygenase 2; KA, kynurenic acid; KYN, L-kynurenine; LC/MS, Liquid Chromatography/Mass spectrometry; mRNA, messenger ribonucleic acid; PCR, polymerase chain reaction; RNA, ribonucleic acid; RT-qPCR, real time quantitative polymerase chain reaction; shRNA – small hairpin RNA; siRNA, small interfering RNA; TCA, trichloroacetic acid; TCDD, 2,3,7,8-tetrachlorodibenzo[p]dioxin; TCGA, The Cancer Genome Atlas; TDO, Tryptophan-2,3-dioxygenase; TNBC, triple negative breast cancer; XA, xanthurenic acid

Molecular Pharmacology Fast Forward. Published on August 29, 2016 as DOI: 10.1124/mol.116.105361
This article has not been copyedited and formatted. The final version may differ from this version.

Abstract

Endogenous ligand-activated AHR plays an important role in numerous biological processes. As the known number of AHR-mediated processes grows, so too does the importance of determining what endogenous AHR ligands are produced, how their production is regulated, and what biological consequences ensue. Consequently, our studies were designed primarily to determine if $ER^-/PR^-/Her2^-$ breast cancer cells have the potential to produce endogenous AHR ligands and, if so, how production of these ligands is controlled. We postulated that: 1) malignant cells produce tryptophan-derived AHR ligand(s) through the kynurenine pathway, 2) these metabolites have the potential to drive AHR-dependent breast cancer migration, 3) the AHR controls expression of a rate-limiting kynurenine pathway enzyme(s) in a closed amplification loop, and 4) environmental AHR ligands mimic the effects of endogenous ligands. Data presented here indicate that primary human breast cancers, and their metastases, express high levels of AHR and TDO; representative $ER^-/PR^-/Her2^-$ cell lines express TDO and produce sufficient intracellular kynurenine and xanthurenic acid concentrations to chronically activate the AHR. TDO over-expression, or excess kynurenine or xanthurenic acid, accelerate migration in an AHR-dependent fashion. Environmental AHR ligands TCDD and B[a]P mimic this effect. AHR knockdown or inhibition significantly reduces *TDO2* expression. These studies identify, for the first time, a positive amplification loop in which AHR -dependent *TDO2* expression contributes to endogenous AHR ligand production. The net biologic effect of AHR activation by endogenous ligands, which can be mimicked by environmental ligands, is an increase in tumor cell migration, a measure of tumor aggressiveness.

Molecular Pharmacology Fast Forward. Published on August 29, 2016 as DOI: 10.1124/mol.116.105361
This article has not been copyedited and formatted. The final version may differ from this version.

Introduction

The aryl hydrocarbon receptor (AHR) is the only ligand-binding member of the evolutionarily conserved (Hahn, 2002) basic Helix-Loop-Helix/Per-Arnt-Sim (bHLH/PAS) family of transcription factors (Hahn, 1998; Hahn, 2002). bHLH/PAS proteins contribute to several important physiological processes, including regulation of circadian rhythm (Garrett and Gasiewicz, 2006), responses to hypoxia (Hirota, 2015; Ichihara et al., 2007), and vascular (Lahvis et al., 2005) and neuronal development (Hester et al., 2007; Huang et al., 2004).

The AHR originally gained notoriety for its role in environmental chemical sensing and metabolism (Ema et al., 1994). However, the known scope of its role in mammalian physiology has quickly expanded as accumulating evidence demonstrates that, like other PAS family members, the AHR plays a critical role in several important biological processes. For example, $AHR^{-/-}$ mice exhibit cardiovascular, hepatic, and reproductive abnormalities (Abbott et al., 1999; Andreola et al., 1997; Barnett et al., 2007; Benedict et al., 2000; Fernadez-Saluero et al., 1997; Fernandez-Salguero et al., 1995; Lahvis et al., 2000; Lahvis et al., 2005; Schmidt et al., 1996; Thackaberry et al., 2002; Vasquez et al., 2003), develop colitis (Fernadez-Saluero et al., 1997) and immune system deficiencies (Fernadez-Saluero et al., 1997; Kerkvliet, 2009; Kimura et al., 2009), and produce hematopoietic stem cells that are prone to stem cell exhaustion. Furthermore, the AHR influences responses to hypoxia (Jensen et al., 2006), TH_{17} and Treg development (Apetoh et al., 2010; Funatake et al., 2005; Gagliani et al., 2015; Quintana et al., 2008), antigen-presentation (Mezrich et al., 2010; Nguyen et al., 2010), and embryonic (Wang et al., 2013b) and hematopoietic (Casado et al., 2011; Smith et al., 2013) stem cell differentiation. Given these findings, it seems likely that aberrant AHR signaling, mediated by exposure to environmental ligands or by excessive production of endogenous ligands, could contribute to multiple pathologic outcomes. Here, we focus on chronic AHR signaling through production of endogenous ligands in breast cancer cells leading to increased tumor cell migration.

Recent evidence suggests that the AHR plays a critical role in cancer progression. The AHR is hyper-expressed and chronically active (Chang and Puga, 1998; DiNatale et al.; Gramatzki et al., 2009; Roblin et al., 2004) in glioblastoma (Gramatzki et al., 2009; Opitz et al., 2011), lymphoma (Sherr and Monti, 2013), T cell leukemia (Hayashibara et al., 2003), and pancreatic (Jin et al., 2015; Koliopanos et al., 2002),

Molecular Pharmacology Fast Forward. Published on August 29, 2016 as DOI: 10.1124/mol.116.105361
This article has not been copyedited and formatted. The final version may differ from this version.

ovarian (Wang et al., 2013a), lung (Chang et al., 2007), liver (Liu et al., 2013), and head and neck carcinoma (DiNatale et al.). A role for the AHR in breast cancer in particular is suggested by: 1) a high level of constitutively active AHR in rodent and human breast cancer models and in primary human tumors (Barhoover et al., 2010; Currier et al., 2005; Goode et al., 2013; Kim et al., 2000; Korzeniewski et al., 2010; Larsen et al., 2004; Li et al., 2014; Schlezinger et al., 2006; Trombino et al., 2000; Wang et al., 1999), 2) a correlation between AHR activity and transcriptional up-regulation of genes associated with invasion (Belguise et al., 2007) and survival (Vogel et al., 2011), 3) AHR-mediated degradation of E-cadherin (Chen et al., 2014), 4) down-regulation of invasion and metastasis-associated genes after *AHR* knockdown (Goode et al., 2014), 5) inhibition of breast cancer cell line invasion, migration, metastasis or mammosphere formation following AHR inhibition (Parks et al., 2014) or knockdown (Goode et al., 2013; Zhao et al., 2013), and 6) acquisition of an invasive phenotype after ectopic expression of *AHR* in non-malignant breast epithelial cells (Brooks and Eltom, 2011). Paradoxically, AHR hyper-activation with exogenous ligands may also lead to reduced breast cancer cell invasion (Hall et al., 2010; Jin et al., 2014; Prud'homme et al., 2010; Safe et al., 2013; Zhao et al., 2012), suggesting that endogenous and exogenous ligands may induce different signaling pathways in a context-specific fashion (Murray et al., 2014; Schlezinger et al., 2006).

The nature and regulation of the endogenous ligands driving “constitutive” AHR activity are poorly understood. Our interest in a possible link between tryptophan metabolism and the AHR in breast cancer stems from the observations that aberrant tryptophan metabolism has long been associated with breast cancer (Bell et al., 1975; Bell et al., 1971; Cascino et al., 1991; Cascino et al., 1995; Chen et al., 2009; Chung and Gadupudi, 2011; Davis et al., 1973; DeGeorge and Brown, 1970; Fahl et al., 1974; Lehrer et al., 1988; Lyon et al., 2011) and that the kynurenine pathway, which accounts for nearly 90% of tryptophan metabolism in humans (Chung and Gadupudi, 2011), is a source of endogenous AHR ligands (Chung and Gadupudi; Heath-Pagliuso et al., 1998; Mezrich et al., 2010; Nguyen et al., 2010; Opitz et al., 2011). The rate-limiting step in the kynurenine pathway is the conversion of L-tryptophan to N-formyl-kynurenine by indoleamine-2,3-dioxygenase 1/2 (IDO1/2) or tryptophan-2,3-dioxygenase (TDO)(Opitz et al., 2011; van Baren and Van den Eynde, 2015). N-formyl-kynurenine is then hydrolyzed to L-kynurenine (KYN), which is metabolized further into kynurenic acid (KA) and xanthurenic acid (XA), all three of the latter being inducers

Molecular Pharmacology Fast Forward. Published on August 29, 2016 as DOI: 10.1124/mol.116.105361
This article has not been copyedited and formatted. The final version may differ from this version.

of AHR activity (DiNatale et al., 2010). Of note, two studies implicated TDO in generating endogenous AHR ligands responsible for tumor invasiveness (D'Amato et al., 2015; Opitz et al., 2011).

The apparent role of the kynurenine pathway in cancer and in AHR activation, combined with the ability of endogenous ligand-activated AHR to contribute to malignancy, lead us to hypothesize that tryptophan metabolites, generated via the IDO1/2 and/or TDO-dependent kynurenine pathway, drive AHR activity and promote tumor cell migration. Furthermore, data from studies investigating the role of the AHR and tryptophan metabolites in the immune system suggest the potential for the AHR to regulate *IDO1/2* transcription and, thereby, production of immunosuppressive tryptophan metabolites (Vogel et al., 2008). Therefore, we further predicted that endogenous (KYN, XA, KA) AHR ligands drive *IDO1/2* or *TDO2* expression and increase production of tryptophan-derived metabolites in a positive feedback loop within the tumor cells, thereby favoring tumor aggressiveness. Cell lines derived from human triple negative ($ER^-/PR^-/HER2^-$)(Hs578T, BP1, MDA-MB-231), triple negative inflammatory (SUM149), or single positive, $Her2^+$ breast cancers, as well as non-malignant mammary epithelial (MCF10F) cells were used to test these predictions. This study focused primarily on ER negative cell lines specifically to observe AHR signaling that is independent of the ER signaling pathway and to determine if either tryptophan oxygenase or the AHR represent viable therapeutic targets in subsets of aggressive breast cancers for which effective targeted therapeutics are lacking.

Materials and Methods

Chemicals

Dimethylsulfoxide (DMSO), 2,3,7,8-tetrachlorodibenzo[p]dioxin (TCDD), tryptophan, KYN, XA acid and KA were obtained from Sigma-Aldrich (St. Louis, MO). Puromycin was purchased from Invitrogen (Grand Island, NY). 6-Formylindolo[3,2-b]carbazole (FICZ) and CH223191 were synthesized and generously provided by Dr. M. Pollastri (Northeastern University).

Cell culture and media

MCF10F and BP1 (invasive tumor-forming cells generated by treatment of MCF10F cells with B[a]P (Calaf and Russo, 1993)) cells were cultured according to ATCC recommendations (ATCC, Manassas, VA)

Molecular Pharmacology Fast Forward. Published on August 29, 2016 as DOI: 10.1124/mol.116.105361
This article has not been copyedited and formatted. The final version may differ from this version.

but without cholera-toxin and with 100 IU/ml penicillin, 100 μg/ml streptomycin (Mediatech) and 5 μg/ml plasmocin (Invivogen, San Diego, CA). MDA-MB-231 and cells were cultured in DMEM Medium (Mediatech, Hernon, VA) containing 10% FCII (Hyclone), 100 IU/ml penicillin, 100 μg/ml streptomycin (Mediatech) and 2 mM L-glutamine (Mediatech). MDA-MB-231-BO cells, a luc-expressing bone-seeking metastatic line derived from the MDA-MB-231 line (Wetterwald et al., 2002; Yoneda et al., 2001), were grown as for MDA-MB-231 cells with the addition of 800 μg/ml of Geneticin (Invitrogen). Hs578T cells, obtained from the ATCC, were cultured in F-12 Medium (Mediatech, Herndon, VA) containing 10% FBS (Sigma-Aldrich), 19.4 mM D-glucose (Sigma, cell culture tested), 100 IU/ml penicillin, 100 μg/ml streptomycin (Mediatech), 5 μg/ml plasmocin (Invivogen), 2 mM L-glutamine (Mediatech) and 10 μg /ml insulin (Sigma). SUM149 cells were maintained in F-12K Medium (Mediatech) containing 5% FBS (Sigma-Aldrich), 0.5 μg/ml hydrocortisone (Sigma-Aldrich), 2 mM L-glutamine (Mediatech), 100 IU/ml penicillin, 100 μg/ml streptomycin (Mediatech), 10 μg/ml insulin (Sigma-Aldrich), and 5 μg/ml plasmocin (Invivogen). HCC202 cells (obtained from ATCC) were maintained in RPMI (Corning) containing 10% FBS according to ATCC recommendations, supplemented wtih 100 IU/ml penicillin and 100 mg/ml streptomycin (Mediatech). Stably transduced Hs578T cells were maintained in culture containing 1.5 μg/ml puromycin and transferred to puromycin-free medium three to five days prior to experiments. Where indicated, cultures were supplemented up to 16 mg/L tryptophan. Culture conditions were maintained at 37^0C, 5% CO_2.

Immunohistochemistry

Immunohistochemistry was performed at the Boston University Immunohistochemistry Core Facility on 5 μm serial sections of paraffin-embedded, invasive breast ductal carcinoma in a tissue microarray (US Biomax, Inc., Rockville, MD) by standard protocol on an intelliPATH Automated Slide Staining System from Biocare Medical (Concord, CA). The array had serial sections (5 μm) primary tissue and matched lymph nodes from 50 cases. After heading slides for 15 minutes at 60 °C, samples were deparaffinization with xylene and rehydrated through graded alcohols to distilled water. The Diva Decloaker (Biocare Medical) reagent was then used for antigen retrieval at 100 °C for 35 minutes, and then at 85 °C for 10 minutes. Slides were incubated with Biocare Medical Peroxidase 1 solution at room temperature for 10 minutes, washed with TBST, blocked with Biocare Medical Background Sniper for 30 minutes and washed. rabbit

Molecular Pharmacology Fast Forward. Published on August 29, 2016 as DOI: 10.1124/mol.116.105361
This article has not been copyedited and formatted. The final version may differ from this version.

AHR-specific antibody (clone H-211, 1:200 dilution, Santa Cruz Biotechnology) or rabbit TDO-specific antibody (clone NBP2-13424, 1:100 dilution, Novus Biologicals, Littleton, CO) was diluted in Da Vinci Green Diluent and incubated at room temperature for 2 hours and washed in TBST (Optimal antibody concentrations were calibrated with sets of normal and malignant tissue). Incubation in Biocare Medical Mach 4 Universal HRP Polymer was then performed for 30 minutes, followed by washing in TBST. DAB was diluted in DAB substrate buffer and applied to slides for 5 minutes, followed by washing in deionized H2O. A light hematoxylin stain was applied, the slides were dehydrated, air dried, and mounted, using EcoMount and a coverslip. Photomicrographs were taken with a Nikon Eclipse microscope connected to a Q Capture Olympus camera and using NIS Elements software. No stain was detectable when substituting rabbit IgG for AHR- or TDO-specific antibody (data not shown).

RT-qPCR

The RNeasy® Plus Mini Prep Kit (Qiagen, Valencia, CA) was used for RNA recovery and cDNA was prepared using the GoScript™ Reverse Transcription System (Promega, Madison, WI) with a 1:1 mixture of oligo $(dT)_{15}$ and random primers. The GoTaq® RT-qPCR Master Mix System (Promega). Was used for RT-qPCR reactions. Validated primers were purchased from Qiagen Inc. (Valencia, CA): human *CYP1B1* - QT00209496, *TDO2* - *QT00027902, 18S* - *QT00225897, IDO1*- QT00000504*, IDO2* - QT01662920. A 7900HT Fast Real-Time PCR instrument (Applied Biosystems, Carlsbad, CA) was used for RT-qPCR reactions with hot-start activation at 95° C for 2 min, 40 cycles of denaturation (95° C for 15 sec) and annealing/extension (55° C for 60 sec). The threshold value for *18S* RNA for normalization and the relative gene expression were determined using the Pfaffl method (Pfaffl, 2001).

For qPCR analysis presented in Supplementary Figure S2, total RNA was extracted using the RNeasy® Plus Mini Kit (Qiagen, Valencia, CA) according to the manufacturer's instructions. Quantitative RT-qPCR analysis was conducted on StepOnePlus™ Real-Time PCR System. Relative mRNA expression was quantified using the comparative Ct (ΔΔCt) method according to the ABI manual (Applied Biosystems, Foster City, CA). Amplification of *18s* was used in each reaction as an internal reference gene. TaqMan probes were used for the human *IDO1 (*Hs00984148_m1) and *18S* (Hs99999901_s1) from the TaqMan®Gene Expression Assays (Applied Biosystems).

Molecular Pharmacology Fast Forward. Published on August 29, 2016 as DOI: 10.1124/mol.116.105361
This article has not been copyedited and formatted. The final version may differ from this version.

Protein extraction and western immunoblotting

Cells were grown to 70% confluence in T75 (75 cm^2) flasks and harvested with trypsin. The cells were lysed in RIPA buffer (Fisher) containing protease and phosphatase inhibitors (Sigma/Aldrich). Immunoblotting was performed as previously described (Parks et al., 2014). Blots were incubated overnight with TDO-(1:1000, SAB1411338, Sigma-Aldrich), AHR- (1:1000, 13790, Cell Signaling), or CYP1B1-(1:1000, sc-32882, Santa Cruz) specific antibody produced in rabbit and with β-actin-specific antibody (1:2000, A5441) (Sigma-Aldrich), to control for loading variability.

Liquid chromatography/mass spectrometry (LC/MS) analysis.

To prepare metabolite extracts from cell lysates, Hs578T cells were cultured in 225 cm^3 flasks for 4 days and metabolite extraction was performed using an 80% (vol/vol) cold methanol extraction method (Yuan et al., 2012). To determine extraction efficiency, a spiked cell lysate sample was prepared by addition of recovery standards after the cells were harvested in ice-cold methanol and transferred to 15 mL conical tubes. To determine sample concentration, titrated doses of recovery standards were dissolved in 80% (vol/vol) cold methanol. Final extracts and standards were lyophilized and stored in -80^o C until further analysis.

For tandem LC/MS analysis, a triple quadrupole linear ion trap mass spectrometer (3200 TRAP, AB Sciex, Foster City, CA), coupled to a binary pump HPLC (1200 Series, Agilent, Santa Clara, CA) was used. Chromatographic separation was achieved based on hydrophilic interaction on an aminopropyl column (Luna 5 μm NH_2 100 Å 250 mm × 2 mm, Phenomenex, Torrance, CA) using a solvent gradient method. Solvent A was a solution of ammonium acetate (20 mM) and ammonium hydroxide (20 mM) in water with 5% acetonitrile (v/v) (pH 9.45)(Bajad et al., 2006). Solvent B was neat acetonitrile. The following gradient was used: t=0, 85% B; t=15 min, 100% B; t=28 min, 100% B; t= 30 min, 15% B; t=50 min, 15% B. Prior to sample analysis, MS parameters were optimized by direct infusion with KYN, XA and KA using commercial metabolite solutions (10 μM in MS-grade DI water). The mass analyzer was operated in negative ion mode for KYN and KA and in positive mode for XA. The following mass transitions were used in the MRM scans and for quantification: KYN: *m/z* 207.0>143.8, KA: *m/z* 187.9>143.8, XA: *m/z* 206.0>160.0.

Molecular Pharmacology Fast Forward. Published on August 29, 2016 as DOI: 10.1124/mol.116.105361
This article has not been copyedited and formatted. The final version may differ from this version.

For sample analysis, each lyophilized cell extract pellet was dissolved in 50-80 μL of MS-grade DI water. Peak identification and integration were performed using Analyst software (version 1.6, ABSciex, Foster City, CA). Sample concentrations were determined from standard curves for each metabolite. Intracellular concentrations were determined using the number of cells from which extracts were prepared and an approximate mammalian epithelial cell volume of 2000 μm^3 (2010; Milo et al., 2010).

Colorimetric kynurenine assay

Collected cell supernatants were stored at -20^0 C until colorimetric analysis. For analysis, 160 μL of supernatant was added to 96-well culture plate and mixed with 10 μL/well of 30% (v/v) freshly prepared trichloroacetic acid (TCA). The plate was incubated at 50^0 C for 30 minutes to hydrolyze N-formyl-kynurenine to kynurenine and then centrifuged at 3000 x g for 10 minutes. Supernatant-TCA solution (100 μL) was transferred to a flat-bottom 96-well black plate and mixed with 100 μL of freshly prepared Ehrlich's reagent (1.2% w/v 4-dimethylamino-benzaldehyde in glacial acetic acid). The plate was incubated for 10 minutes at room temperature and absorbance was read with a microplate reader at 492 nm. Culture medium that was not exposed to cells was used as time 0 supernatant.

Stable cells expressing sh*TDO2* and *TDO2*

Lentivirus preparation and transduction were performed according to the manufacturer's protocol. Lentivirus-based *TDO2* shRNA (TRCN0000064900), control plasmid (SHC016 1EA) and lentiviral packaging mix were purchased from Sigma (St. Louis, MO, USA). *TDO2* Lentiviral Vector (pLenti-GIII-CMV-Human-TDO2-GFP-2A-Puro Lentiviral Vector, LV332282) was purchased from Applied Biological Materials Inc. **(**Richmond, BC**.** CANADA). Control, sh*TDO2*, or *TDO2* plasmids were co-transfected with the packaging plasmids into 293T cells using Lipofectamine 2000 (Invitrogen, Carlsbad, CA). Forty-eight hours after transfection, the virus-containing supernatants were harvested and centrifuged at 3,000 rpm for 15 min, and filtrated through a 0.45 μm low protein-binding filter (Millipore, Bedford, MA). Hs578T and SUM149 cells were infected with lentivirus (3 MOI) in the presence of hexadimethrine bromide **(**5 μg/mL polybrene, Sigma-Aldrich) and fed with fresh complete medium the next day. Seventy-two hours after infection, the transduced cells were selected by puromycin (2 μg/ml). Efficiency of TDO knockdown or

Molecular Pharmacology Fast Forward. Published on August 29, 2016 as DOI: 10.1124/mol.116.105361
This article has not been copyedited and formatted. The final version may differ from this version.

overexpression was validated by qRT-PCR and immunoblot analyses. Cells were cultured thereafter in 1.5 μg/ml puromycin, and changed to puromycin-free medium three to five days prior to each experiment.

Stable, doxycycline-inducible *AHR*-specific shRNA-expressing cells

Viral transduction particles were generated with a doxycycline (dox)-inducible *TurboRFP-shAHR* TRIPZ lentiviral vector (Open Biosystems, Huntsville, AL). Hs578T cells were transduced at an optimal MOI of 25 in medium containing hexadimethrine bromide (8 μg/mL polybrene; Sigma-Aldrich). Transduced cells were maintained in 1.5 μg/ml puromycin (Invitrogen, Grand Island, NY). Red Fluorescent Protein (RFP) expression was maximal 48 hours after dox treatment (1.5 μg/ml) of transduced cells.

CRISPR-Cas9-mediated AHR deletion in MDA-MB-231 cells.

The CRISPR expression vector lentiCRISPR v2 (Addgene no. 52961) containing hCas9 and single strand guide RNA (sgRNA), was digested with BsmBI. A pair of annealed human *AHR* oligonucleotides were cloned into the guide RNA scaffold as described (Sanjana et al., 2014). The two target sites are located in the first exon of the *AHR* [5'-CCTACGCCAGTCGCAAGCGG and 5'-CCGAGCGCGTCCTCATCGCG, NM_001621)]. To rule out off-target effects, the guide RNA sequence was searched using an online-based web tool (http://genome-engineering.org/). MDA-MB-231 cells were infected with *AHR* lentiCRISPR v2-Cas9-sgRNA lentivirus, according to the standard protocol (Sanjana et al., 2014). Cells were selected for 10 days with 2.0 μg/ml puromycin. AHR knockout was confirmed by Western blotting as previously described (Stanford et al., 2016a) and direct qPCR sequencing.

Transient transfection

MCF10F cells (2 x 10^4 in 500 μL complete medium) were plated in a 24-well plate, allowed to adhere overnight and co-transfected with the AHRE-driven firefly luciferase reporter construct *pGudluc* (1 μg/mL) (generously provided by Dr. M. Denison, UC, Davis) and *CMV-green* (0.5 μg/mL) using TransIT-2020 transfection reagent (Mirus, Madison, WI*).* Aftere 24 hours, the medium was replaced. Cells were left untreated or dosed with vehicle (DMSO, 0.1%), titrated doses of KYN, KA or XA, or CH223191 (10 μM) and harvested after 24 hours in Glo Lysis Buffer (Promega, San Luis Obispo, CA). Luciferase activity was determined with the Bright-Glo Luciferase System according to the manufacturer's instructions (Promega). Luminescence and fluorescence were determined using a Synergy2 multifunction plate reader (Bio-Tek,

Molecular Pharmacology Fast Forward. Published on August 29, 2016 as DOI: 10.1124/mol.116.105361
This article has not been copyedited and formatted. The final version may differ from this version.

Winooski, VT). sh*TDO2*-expressing Hs578T cells were transiently transfected with *pGudLuc* and *CMV-green* 24 hours after plating and luminescence was determined 24 hours later, as described above.

For transient siRNA-mediated *TDO2* knockdown, Hs578T cells were transfected with 5 nM of each of two *TDO2*-directed siRNA duplex constructs (5'-GCAGCGAAGAAGACAAAUCACAAAC-3' and 5'-CCACUUAAUGUAAUCACUAUCUCAT-3') or 10 nM scrambled siRNA duplex (5'-CGUUAAUCGCGUAUAAUACGCGUAT-3'). Fresh medium was added 24 hours later. Cells then were transfected with *pGudluc* and *CMV-green,* as above, and luminescence determined 24 hours later.

Scratch-Wound Assay

Confluent monolayers of SUM149 cells were pre-treated in 6-well plates with vehicle (0.1% DMSO), 10-100 μM XA, 50-100 μM KYN, 0.5 μM FICZ, 1 μM B[a]P, or 1 nM TCDD with or without 10 μM CH223191, serum-starved for 24 hours, scratched with a p200 pipette tip, and washed with PBS to remove non-adherent cells. Photographs were taken at the same location relative to the scratch at time 0 and every day thereafter. The media was changed and cells were re-dosed daily. TScratch software (Tobias Gebäck and Martin Schulz, ETH Zürich) was used to quantify the closure of the scratch over time. None of these treatments affected cell viability or cell proliferation rates as determined by MTT assays.

Gene Expression Preprocessing

Fifty eight breast cancer cell lines from the Cancer Cell Line Encyclopedia (CCLE) containing Affymetrix U133 Plus 2.0-based transcriptomic information (Barretina et al., 2012) were used to assess correlations between *AHR* and *CYP1B1* expression. These data were normalized using Robust Multi-Array Average (Irizarry et al., 2003) using the R/Bioconductor (Team, 2012) package 'affy', with raw probe levels mapped to Ensembl gene identifiers based on the custom Brainarray chip definition files (CDF) (Dai et al., 2005). Similarly, transcriptomic information from 977 primary mammary epithelial tumor samples and adjacent "normal" tissue from The Cancer Genome Atlas (Cancer Genome Atlas, 2012) were used. The TCGA portal provides level 3, FPKM-normalized count data, which were used to determine relative *TDO2* mRNA levels and to analyze correlations between *AHR* and *CYP1B1* within primary tissues. TCGA provides immunohistochemistry data on estrogen, progesterone and Her2 receptor status, as well as tissue sample status (tumor vs. adjacent "normal" tissue) and tumor stage data, which were used to stratify the

Molecular Pharmacology Fast Forward. Published on August 29, 2016 as DOI: 10.1124/mol.116.105361
This article has not been copyedited and formatted. The final version may differ from this version.

data based on ER, Progesterone and Her2 receptor status or on staging. All Pearson correlations, false discovery rate (FDR) corrections and plots were performed using the statistical programming language R.

For *TDO2* expression analyses, TCGA data were retrieved from level three RNA_{Seq} version 2. Transcript abundance was estimated by RNA-Seq by Expectation Maximization (RSEM) package (Li and Dewey, 2011). RSEM estimated values were normalized using sample specific scaling factors (75% percentile) and multiplied by 1000. An added pseudo-count of one was used to compare log_2-normalized expression of *TDO2* in tumor versus tumor-adjacent normal samples. The p values for *TDO2* expression comparisons were calculated using Welch's unequal variances *t*-test in R.

Statistical analyses

Statistical analyses were performed with Prism (GraphPad Software, La Jolla, CA) or StatPlus (Alexandria, VA). Data are presented as mean + standard error (SEM) where applicable. One-way analysis of variants (ANOVAs) (simple) or Student's T-test was used as indicated to determine significance.

Results

AHR and TDO expression in Human Breast Cancer

Previous studies demonstrate that the AHR is "constitutively active" in several different types of cancers (Barhoover et al., 2010; Chang and Puga, 1998; Chang et al., 2007; Currier et al., 2005; DiNatale et al., 2011; Korzeniewski et al., 2010; Roblin et al., 2004; Trombino et al., 2000; Yang et al., 2005; Yang et al., 2008) and that it may play a role in tumor invasion and/or migration (Brooks and Eltom, 2011; Dietrich and Kaina, 2010; Diry et al., 2006; Goode et al., 2013; Gramatzki et al., 2009; Schlezinger et al., 2006). In triple negative breast cancer (TNBC) cell lines, this high baseline AHR activity enforces expression of a prototypic AHR target gene, *CYP1B1* (Yang et al., 2008). Indeed, a significant positive correlation can be seen between *AHR* and *CYP1B1* levels in 58 mammary epithelial cancer cell lines annotated in the Cancer Cell Line Encyclopedia (CCLE) dataset (FDR = 3.8×10^{-7}) and in 977 mammary tumors represented in the TCGA dataset (FDR < 3×10^{-16})(Figure 1) suggesting that the AHR is constitutively active in human breast cancers in general, presumably because of the presence of endogenous ligands, and that *CYP1B1* expression is a useful surrogate marker for AHR expression and/or activity.

Molecular Pharmacology Fast Forward. Published on August 29, 2016 as DOI: 10.1124/mol.116.105361
This article has not been copyedited and formatted. The final version may differ from this version.

Similarly, immunohistochemical analysis of 50 human breast cancers and patient-matched lymph node (LN) metastases demonstrated strong AHR staining within malignant cells in both the primary tumor and the LN metastases (Figure 2). The AHR stain was consistently localized to cell nuclei (red arrows, Figure 2) in both $ER^-/PR^-/Her2^-$ tumors (e.g., left panels) and ER^+ tumors (e.g., right panels), a result consistent with "constitutive" AHR activity in breast cancers. TDO staining also was strong in these 50 primary tumor and metastases samples, with AHR and TDO staining tending to co-localize within the tumor (compare top to bottom panels).

Analysis of the TCGA database revealed that primary breast cancers express dramatically elevated levels of *TDO2* mRNA as compared with histologically normal adjacent normal ("AN") tissue, regardless of estrogen, progesterone or Her2 receptor status (Figure 3A, $p<0.001$). TNBC tumors express significantly higher *TDO2* than ER^+ tumors (Figure 3A, $p<0.001$). Interestingly, normal tissue adjacent to TNBC tumors expresses modestly higher *TDO2* levels than the corresponding adjacent normal tissue from ER^+ tumors (Figure 3A)($p<0.05$) suggesting a subtle but possibly important field effect in which *TDO2* is higher in tissue surrounding more aggressive breast cancers. When samples were segregated according to tumor staging, it can be seen that tumors at stages 1-3 express significantly higher *TDO2* than adjacent normal tissue (Figure 3B). *TDO2* expression in Stage 4 tumors is also higher than adjacent normal tissue, although sample size of adjacent normal tissue (2 samples) precluded statistical analysis (Figure 3B). Furthermore, stage 4 breast cancers express significantly higher *TDO2* mRNA than stage 3 tumors ($p<0.05$), again suggesting that the highest *TDO2* levels characterize the most aggressive cancers.

TDO expression and influence on AHR activity

Despite what appears to be a generalizable elevation of AHR expression and activity in breast cancers, and the potential for the AHR to play a significant role in mediating breast cancer invasion and/or migration, at least in ER^- cells (Brooks and Eltom, 2011; Chen et al., 2014; Goode et al., 2014; Goode et al., 2013; Li et al., 2014; Parks et al., 2014), the exact nature of and mechanisms responsible for production of endogenous AHR ligands that drive AHR activity in breast cancer have not been established. Recent studies implicate tryptophan metabolites produced via the kynurenine metabolic pathway in tumor progression (Opitz et al., 2011) and in AHR activation (DiNatale et al., 2010; Mezrich et al., 2010; Nguyen et al., 2010). Therefore, we hypothesized that proximal, rate-limiting enzymes in the kynurenine pathway,

Molecular Pharmacology Fast Forward. Published on August 29, 2016 as DOI: 10.1124/mol.116.105361
This article has not been copyedited and formatted. The final version may differ from this version.

TDO and/or IDO1/2, regulate AHR signaling and TNBC functionality by facilitating endogenous AHR ligand production.

To determine which, if any, of these enzymes is expressed in human mammary epithelial cell lines, *TDO2*, *IDO1*, *and IDO2* mRNA levels were quantified by RT-qPCR in a non-malignant mammary epithelial cell line (MCF10F), four TNBC cell lines (BP1, Hs578T, MDA-MB-231, and MDA-MB-231-BO), and in an inflammatory breast cancer cell line (SUM149). Only one line, MDA-MB-231, produced detectable levels of *IDO1* mRNA (after 30 cycles) and no lines expressed detectable *IDO2* mRNA (not shown). Little to no *TDO2* was detected in MCF10F and SUM149 cells (Figure 4A). BP1, MDA-MB-231, and MDA-MB-231-BO cells consistently expressed low *TDO2* levels detected at 30-32 cycles. In contrast, Hs578T cells expressed 46-fold more *TDO2* than MCF10F cells. TDO protein levels roughly correlated with *TDO2* mRNA expression in these cell lines, with Hs578T cells exhibiting approximately 57-fold more TDO protein than MCF10F cells (Figure 4B and C). Therefore, Hs578T cells, which more closely reflected elevated AHR and TDO expression in primary tumors (Figures 2 and 3) were selected for the next series of experiments.

To determine if TDO influences AHR activity, presumably through production of endogenous ligands, *TDO2* was down-regulated by stable transduction of Hs578T cells with *TDO2*-specific shRNA (sh*TDO2*) or by transient transfection with *TDO2*-specific siRNA. *TDO2* levels were quantified by RT-qPCR to confirm knockdown, *CYP1B1* levels were quantified as a surrogate marker for endogenous gene-specific AHR activity (Yang et al., 2008), and *pGudLuc* reporter activity was assayed as a more general measure of AHR activity. Stable expression of sh*TDO2* significantly reduced *TDO2* levels by 83% ($p<0.05$), endogenous *CYP1B1* levels by 31% ($p<0.01$), and *pGudLuc* activity by 37% ($p<0.05$)(Figure 5A, B, C). Similarly, transient transfection with *TDO2*-specific siRNA significantly reduced *TDO2* levels by 49% ($p<0.001$), *CYP1B1* expression by 24% ($p<0.05$), and *pGudLuc* activity by 17% ($p<0.05$)(Figure 5D, 5E, 5F). These data indicate that TDO is at least partially responsible for baseline (constitutive) AHR activity in Hs578T tumor cells.

Hs578T cells produce physiologically relevant levels of kynurenine and xanthurenic acid, two endogenous AHR ligands

The contribution of TDO to AHR activity led us to hypothesize that tryptophan metabolites of the kynurenine pathway are produced in Hs578T cells and drive constitutive AHR activity. It has been reported

Molecular Pharmacology Fast Forward. Published on August 29, 2016 as DOI: 10.1124/mol.116.105361
This article has not been copyedited and formatted. The final version may differ from this version.

that at least three kynurenine pathway metabolites, kynurenine (KYN), xanthurenic acid (XA), and kynurenic acid (KA), are either AHR ligands or precursors to AHR ligands in human glial cells and hepatocytes (DiNatale et al., 2010; Opitz et al., 2011). To determine if and at what concentrations these three tryptophan metabolites activate the AHR in human mammary epithelial cells, MCF10F cells, which exhibit relatively low baseline AHR-dependent *pGucLuc* activity (data not shown) and express little to no *TDO2* or *IDO1/2* (Figure 4 and data not shown), were treated with titered doses (0.1- 400 μM) of KYN, XA or KA and *pGudLuc* reporter activity was assayed 24 hours later. As expected, KYN, XA and KA induced AHR activity in a dose-dependent manner with EC_{50}s of 7.02 μM, 127 μM and 180 μM, and maximal fold induction of 2.6, 3.7 and 1.8, respectively (Figure 6). Induction of *pGudLuc* activity was significantly inhibited by an AHR-specific antagonist, CH223191 (Figure 6). Importantly, KYN tended to induce AHR activity at 1-5 μM and produced a maximal increase in pGudLuc reporter activity at 50 μM ($p<0.01$), a concentration within the range of the previously reported KYN concentrations in human tumors and sera of cancer patients (Lyon et al., 2011; Opitz et al., 2011). Furthermore, XA induced significant AHR reporter activity at a dose as low as 1 μM ($p<0.05$). These results support the hypothesis that TDO-derived tryptophan metabolites KYN, XA and possibly KA can induce AHR activity in mammary epithelial cells, with KYN and XA demonstrating the highest potency and efficacy.

LC/MS was used to determine if KYN, XA and KA are present in Hs578T cells at concentrations sufficient to activate the AHR. All three metabolites were detected in Hs578T cell lysates (Figure 7A). Intracellular metabolite concentrations were determined to be 90.3 μM for KYN, 4.5 μM for XA and 0.52 μM for KA (Figure 7B). Both the KYN and XA concentrations are sufficient to induce a significant ~1.5-2.5-fold increase in AHR reporter activity in mammary epithelial cell lines (Figure 6). To our knowledge, this is the first demonstration of the production of physiologically relevant intracellular concentrations of KYN and XA by breast cancer cells. Furthermore, the intracellular KYN levels reported here in breast cancer cells are approximately 90 times greater than the secreted KYN levels previously reported (D'Amato et al., 2015).

Since KYN and its metabolites are likely to accumulate in the media, as they do in the tumor microenvironment (Chen et al., 2014; Opitz et al., 2011), a rapid colorimetric method for measuring KYN in supernatants (Hara et al., 2008; Lee et al., 2014) was used to quantify the accumulation of KYN in culture

Molecular Pharmacology Fast Forward. Published on August 29, 2016 as DOI: 10.1124/mol.116.105361
This article has not been copyedited and formatted. The final version may differ from this version.

supernatants over 92 hours. Indeed, a gradual increase in KYN concentration in Hs578T cell supernatant was observed over a 92 hour period with the concentration peaking at approximately 3 times the initial concentration by 92 hours (Figure 8A, left panel). LC/MS analysis indicated levels of KYN in supernatant at 92 hours (150 μM)(Figure 8A) sufficient to activate the AHR (Figure 6). As would be expected from the relative levels of TDO and IDO in SUM149 cells (Figure 4, no detectable TDO or IDO protein or mRNA), no KYN accumulation was detected in supernatants of SUM149 cells (Figure 8A, middle panel). A modest 2-fold increase in KYN accumulation was seen with MDA-MB-231 cells (Figure 8A, right panel), a cell line that expresses low TDO and IDO (Figure 4 and data not shown).

Since Hs578T, SUM149, and MDA-MB-231 cells are grown in different media with different levels of tryptophan (9, 4, and 16 mg/L respectively), Hs578T and SUM149 cultures were spiked with tryptophan to bring the final concentration up to 16 mg/ml and KYN accumulation over 96 hours assayed. (The amount of tryptophan provided by 10% FBS, ~0.6 mg/L, is small compared to the amounts provided by the enriched media). As expected, KYN accumulation in cultures of Hs578T cells, which express high TDO levels, increased over time (Figure 8A, left panel) while no KYN accumulation was observed in cultures of SUM149 cells (Figure 8A, middle panel), which do not express detectable TDO or IDO. Therefore, it is concluded that KYN production is a function of both the levels of TDO/IDO and tryptophan concentration. From this conclusion it would be predicted that TDO down-regulation would reduce KYN production. Indeed, down-regulation of *TDO2* by stable transduction with *TDO2*-specific shRNA (Figure 5A) significantly ($p<0.01$) inhibited KYN accumulation in supernatants (Figure 8B). Collectively, these results demonstrate the ability of breast cancer cells to accumulate physiologically relevant intra- and extra-cellular concentrations of AHR ligands in a TDO-dependent process.

The role of TDO, AHR, and TDO-dependent endogenous AHR ligands in tumor cell migration

It has been suggested that the AHR plays a role in cell migration and metastasis (Brooks and Eltom, 2011; Goode et al., 2014; Goode et al., 2013). Therefore, it would be predicted that TDO over-expression would increase baseline levels of KYN, increase AHR activity, and accelerate cancer cell migration. Inflammatory breast cancer-derived SUM149 cells, which do not express detectable levels of *TDO2* or *IDO1/2* and do not produce detectable levels of KYN (Figures 4 and 8), were used to test this prediction. Indeed, ectopic *TDO2* expression in SUM149 cells significantly increased the accumulation of KYN in

Molecular Pharmacology Fast Forward. Published on August 29, 2016 as DOI: 10.1124/mol.116.105361
This article has not been copyedited and formatted. The final version may differ from this version.

culture supernatants (Figure 9A), increased pGudLuc activity (Figure 9B) and accelerated migration (Figure 9C and D). In all cases, migration was slowed by addition of AHR inhibitor CH223191 (Figure 9D). AHR inhibition had no effect on cell proliferation as assayed by an MTT assay or on cell viability/apoptosis as assayed by propidium iodide incorporation under isotonic (cell death) and hypotonic (apoptosis) conditions (Stanford et al., 2016b) (data not shown). In the case of CH223191 treatment of *TDO2*-transfected cells, the failure to slow migration to the levels seen in wildtype cells treated with CH223191 may reflect either that CH223191, under these conditions, does not inhibit 100% of the AHR-dependent activity or that at least some of the TDO effect is AHR independent. Collectively, these data demonstrate at least partial regulation of tumor cell migration by both AHR and TDO.

To directly determine if the more abundant kynurenine pathway metabolites, KYN or XA, accelerate tumor cell migration, SUM149 cells were grown to confluence, monolayers scratched, and cultures treated with titered doses of KYN, XA or metabolite plus AHR inhibitor. Wound closure was then quantified 36 hours later. Treatment with 100 μM XA or KYN alone significantly accelerated cell migration (Figure 10A and 10B, histograms on left, $p<0.001$ and $p<0.01$ respectively). Addition of 10 μM CH223191 to XA or KYN-treated cultures significantly decreased cell migration ($p<0.0001$) (Figure 10 B), demonstrating AHR dependence. Note that the individual KYN and XA concentrations used are either less than (KYN) or approach (XA) the concentrations of each metabolite present in the tumor cells (Figure 7). 10 μM XA failed to increase cell migration while 50 μM KYN increased migration by 51% but did not reach statistical significance (Figure 10 B). Interestingly, a combination of 10 μM XA and 50 μM KYN significantly accelerated cell migration by 87% (Figure 10B, histograms on right)($p<0.001$). This accelerated migration was dramatically inhibited by CH223191. These data suggest that the presence of two (or more) AHR ligands, as is likely within the tumor environment, induces a more profound, AHR-dependent biologic effect than either metabolite alone.

Collectively, these results demonstrate that both the AHR and TDO influence cell migration rates and support the hypothesis that TDO contributes to cell migration by producing endogenous AHR ligands derived from the kynurenine pathway.

Molecular Pharmacology Fast Forward. Published on August 29, 2016 as DOI: 10.1124/mol.116.105361
This article has not been copyedited and formatted. The final version may differ from this version.

Environmental AHR ligands accelerate tumor migration

The ability of endogenous AHR ligands to accelerate cell migration suggests the possibility that environmental AHR ligands, some of which have been associated with breast cancer incidence (Brody et al., 2007; Manuwald et al., 2012; Revich et al., 2001; Warner et al., 2002; Warner et al., 2011), similarly affect tumor cell migration. To test this prediction, SUM149 cells were grown to confluence, cell monolayers scratched, and cultures treated with: **1)** 0.5 μM 6-formylindolo[3,2-b]carbazole (FICZ), a tryptophan photo-metabolite and high affinity AHR ligand, **2)** 1 μM benzo[a]pyrene (B[*a*]P), a prototypic PAH and carcinogenic environmental AHR ligand (Russo et al., 1993), exposure to which correlates with breast cancer incidence (Li et al., 1999), or **3)** 1 nM 2,3,7,8-tetrachlorodibenzo[p]dioxin (TCDD), a persistent, high affinity environmental AHR ligand, exposure to which is associated with an increased incidence of breast cancer (McGregor DB1, 1998). Notably, FICZ tended increase cell migration by approximately 50%. B[*a*]P and TCDD significantly accelerated wound closure (86%, $p<0.001$ and 67%, $p<0.01$ respectively)(Figure 11). These results demonstrate that different classes of environmental AHR ligands have the capacity to mimic endogenous AHR ligands in their ability to increase cell migration.

The AHR regulates TDO levels

The AHR can control IDO1 expression in non-malignant, murine dendritic cells (Nguyen et al., 2010; Vogel et al., 2008). However, AHR regulation of either IDO or TDO in breast cancer cells has never been shown. To determine if the AHR regulates *TDO2* in human malignant mammary cells, AHR expression or activity was down-regulated in triple negative Hs578T cells, which express relatively high TDO levels (Figure 4), and in triple negative BP1 cells, which express low but detectable TDO levels, with a doxycycline-inducible *AHR*-specific shRNA and/or with CH223191. *AHR* knockdown and/or AHR inhibition significantly reduced *TDO2* expression in both Hs578T and BP1 cells ($p<0.05$) (Figure 12). Similar results were obtained in two independent experiments performed with $HER2^+$ HCC202 cells (Supplementary Figure S1). These results demonstrate, for the first time, that AHR activity plays a significant role in maintaining *TDO2* expression in breast cancer cells in what appears to be an amplification loop that mediates a relatively high level of tumor cell migration.

Molecular Pharmacology Fast Forward. Published on August 29, 2016 as DOI: 10.1124/mol.116.105361
This article has not been copyedited and formatted. The final version may differ from this version.

Since MDA-MB-231 cells express low but detectable *IDO1* levels we were able to test the hypothesis that *IDO* is regulated, at least in part, by the AHR as it is in antigen presenting cells. To test this hypothesis an AHR knockout MDA-MB-231 subline was created by CRISPR-Cas9 technology. This line expressed no detectable AHR or CYP1B1 (Supplemental Figure S2A), indicating that CYP1B1 expression is controlled to a dominant extent by baseline levels of AHR activity. Furthermore, AHR hyper-activation with FICZ induced a strong CYP1B1 signal in control lines but not in the AHR knockout line, indicating a profound diminution or deletion of AHR expression. Importantly, *IDO1* mRNA was significantly lower in the AHR knockout line than in the CRISPR-Cas9 control line (Supplemental Figure S2B). These data are consistent with those in dendritic cells demonstrating AHR control of IDO (Nguyen et al., 2010) and in the Hs578T, BP1, and HSC202 lines with regard to AHR control of *TDO2* (Figure 12 and Supplemental Figure S1).

Discussion

Over much of the last 30 years, the AHR was studied as a regulator of environmental chemical toxicity and carcinogenicity. But in the last 10 years an appreciation has grown for the effects that it has on a number of normal physiological processes (Abbott et al., 1999; Benedict et al., 2000; Bunger et al., 2003; Fernadez-Saluero et al., 1997; Garrett and Gasiewicz, 2006; Lahvis et al., 2005; Schmidt et al., 1996; Thackaberry et al., 2002; Vasquez et al., 2003; Xu et al., 2010). As the known number of these AHR-mediated processes grows, so too does the importance of determining which endogenous AHR ligands are produced and how their production is regulated in pathological processes, including breast cancer, where aberrant AHR activity has been implicated. The studies presented here were directed towards understanding what endogenous AHR ligands are produced by aggressive triple negative and inflammatory breast cancers and how production of these ligands is controlled.

Previous studies strongly suggest a link between elevated AHR expression or activity and cancer progression in the absence of exogenous ligands (i.e, “constitutive” endogenous ligand-driven AHR activity) (Andersson et al., 2002; Chang et al., 2007; D'Amato et al., 2015; Gramatzki et al., 2009; Opitz et al., 2011; Trombino et al., 2000; Yang et al., 2008). Some of these studies were performed *in vitro* with cloned cell lines (Brooks and Eltom, 2011; Goode et al., 2013; Yang et al., 2008) suggesting that

Molecular Pharmacology Fast Forward. Published on August 29, 2016 as DOI: 10.1124/mol.116.105361
This article has not been copyedited and formatted. The final version may differ from this version.

functionally relevant concentrations of endogenous AHR ligands can be produced by malignant cells themselves. If confirmed, then aberrant production of endogenous AHR ligands by transformed cells, or cells of the tumor microenvironment, would represent the most proximal event in a signaling pathway that mediates lethal progression to a metastatic disease.

While several endogenous molecules either activate the AHR or give rise to AHR-inducing metabolites AHR (DiNatale et al., 2010), evidence for their contribution to specific biological outcomes has only begun to be generated (DiNatale et al., 2010; Opitz et al., 2011). Kynurenine pathway metabolites represent promising candidates as contributors to several documented AHR-dependent biological processes, including breast cancer progression which has been associated with aberrant tryptophan metabolism (Bell et al., 1975; Bell et al., 1971; Chen et al., 2009; Davis et al., 1973; DeGeorge and Brown, 1970; Fahl et al., 1974; Girgin et al., 2009; Lehrer et al., 1988; Tang et al., 2014), accumulation of KYN in patient sera (Lyon et al., 2011), and elevated TDO and/or IDO1/2 (Do et al., 2014; Opitz et al., 2011; Pilotte et al., 2012; Sakurai et al., 2005; Travers et al., 2004; Uyttenhove et al., 2003). That said, no other studies have directly quantified intracellular levels of kynurenine, xanthurenic acid, and kynurenic acid specifically within malignant breast cells. Importantly, KYN levels within tumor cells (93 μM) and in tumor cell supernatants (150 μM), as quantified here, and KYN levels in breast cancer patient sera characterized elsewhere (2.3 ± 1.1 μM) (Lyon et al., 2011) approach those shown to be capable of activating the AHR in mammary epithelial cells (Figure 6). This is in contrast to a previous study in which only 1 μM KYN, a dose insufficient to activate the AHR (Figure 6), was detected in breast cancer cell supernatants (D'Amato et al., 2015). Furthermore, intracellular XA levels (4.5 μM) were shown here to be sufficient to activate the AHR.

TDO expression in primary tumors (Figures 2 and 3) raises suspicions about its role in breast cancer since, unlike IDO, TDO is predominantly expressed in liver and not in healthy mammary tissue (Chen and Guillemin, 2009; Opitz et al., 2011; Pilotte et al., 2012). Indeed, *TDO2* expression is significantly higher in tumors than adjacent non-malignant tissue, in triple negative as compared with ER^+ tumors, and in stage 4 as compared with stage 3 tumors (Figure 3), suggesting that high TDO levels may represent a biomarker for aggressive breast cancers. Elevated TDO/IDO expression documented in other cancer types (Brandacher et al., 2006; Chevolet et al., 2014; Choe et al., 2014; Pilotte et al., 2012; Smith

Molecular Pharmacology Fast Forward. Published on August 29, 2016 as DOI: 10.1124/mol.116.105361
This article has not been copyedited and formatted. The final version may differ from this version.

et al., 2012; Theate et al., 2015), suggests that our findings may be relevant to other cancer subtypes as well.

Among a panel of 6 triple negative epithelial cell lines studied, TDO was most elevated in malignant Hs578T cells (Figure 4) in which KYN, and its product XA, are present at concentrations (93.3 μM and 4.5 μM, respectively) capable of AHR activation (5-10 μM and 1-5 μM, respectively)(Figure 6). (KYN contributes to cell invasion in a similar range (50 μM) in glioblastoma (Opitz et al., 2011)). As expected, TDO knockdown significantly reduced accumulation of KYN (Figure 8B), confirming that TDO activity represents a major contributor to baseline production of these AHR ligands. These results suggest that TDO may be as or more important to breast cancer biology than IDO, although significantly more is known of IDO expression in other cell types (Braun et al., 2005; Choe et al., 2014; Hwang et al., 2005; Mellor and Munn, 2004; Staudacher et al., 2015; Yeung et al., 2015). Studies in MDA-MB-231 cells, in which low levels of IDO were detected, indicate that the AHR may similarly control IDO expression in breast cancer (Supplemental Figure S2).

Interestingly, cells that express little or no TDO or IDO (e.g., SUM149, MCF10F) still exhibit a significant baseline level of AHR activity which is inhibited with CH223191 (supplemental Figure S3) or AHR knockdown (not shown), suggesting that non-kynurenine-derived AHR ligands are being made by the tumor cells and/or that the cultures contain AHR ligands from exogenous sources. LC/MS analysis failed to detect FICZ in any of our cultures. However, 1.92 μM and 2.7 μM indoxyl sulfate was detected in Hs578T cell lysates and culture supernatants respectively (data not shown). Indoxyl sulfate is an AHR ligand (Schroeder et al.; Shivanna et al., 2016) that, in our hands, induces AHR activity in MCF10F cells in the 1-5 μM range (data not shown). It's source, in these cultures, appears to be FBS which contains ~9 μM indoxyl sulfate (data not shown).

Data showing that AHR inhibitors slow cell migration (Figure 10)(Barouki et al., 2007; DiNatale et al., 2012; Goode et al., 2013; Lahoti et al., 2014) are consistent with the hypothesis that AHR activity drives a required step in the progression to an aggressive phenotype (van Zijl et al., 2011). Since AHR activity is influenced by TDO-dependent endogenous AHR ligands, it was predicted that TDO expression would correlate with AHR activity and the rate of cell migration. This hypothesis was supported by a

Molecular Pharmacology Fast Forward. Published on August 29, 2016 as DOI: 10.1124/mol.116.105361
This article has not been copyedited and formatted. The final version may differ from this version.

correlation in TDO and AHR expression in primary tissues (Figure 2), increased AHR activity and accelerated migration after ectopic TDO expression *in vitro* (Figure 9), and accelerated migration after addition of KYN and XA *in vitro* (Figure 10).

We show that AHR knockdown with shRNA or suppression of AHR activity with CH223191 significantly reduces *TDO2* mRNA expression in three cell lines. This result is reminiscent of the influence of the AHR on IDO expression in antigen-presenting cells (Nguyen et al., 2010) and uniquely demonstrates a positive feedback loop within breast cancer cells (Visual Abstract). Interestingly, there are no consensus (5-GCGTG-3') or alternative binding sites (5'-GGGAGGGAGGGAGGGA-3' and 5'-GGGTGCAT-3', targeted by AHR/RelB or AHR/Klf6 dimers respectively) within 3,000 base pairs upstream or 200 base pairs downstream of the *TDO2* start site. Therefore, the AHR may regulate *TDO2* expression indirectly, potentially by recruiting the glucocorticoid receptor co-activator SRC1/NCoA1 (Endler et al., 2014) and enhancing glucocorticoid receptor-mediated *TDO2* transcription (Soichot et al., 2013).

The putative amplification loop may be sustained by AHR ligands produced within a given malignant cell, by adjacent malignant cells, and/or by non-malignant cells of the surrounding tumor microenvironment. A modest but consistent level of TDO-specific staining in the microenvironment of primary human breast cancers and their metastases, as seen by immunohistochemistry, is consistent with a contribution of the microenvironment in the postulated amplification loop. In that vein, KYN accumulates in the tumor microenvironment (Puccetti et al., 2015) where it can act in a "paracrine" manner in breast (Chen et al., 2014) and other cancers (Opitz et al., 2011). As such, this autocrine/paracrine communication network may represent a novel route through which malignant cells and cells of the tumor microenvironment perpetuate tumor aggressiveness.

One important implication of results presented here is the suggestion that environmental AHR ligands mimic endogenous ligands and enhance tumor cell migration. Both TCDD, a poorly metabolized and persistent AHR ligand, and B[a]P, a readily metabolized ligand, accelerated migration *in vitro*. Therefore, relatively common environmental AHR ligands could initiate or exacerbate the self-perpetuating AHR-TDO feedback loop, maximizing cell migration.

In conclusion**,** our data demonstrate, for the first time, a complete amplification loop in $ER^-/PR^-/Her2^-$ breast cancer cells through which the AHR drives production of TDO, which generates endogenous AHR

Molecular Pharmacology Fast Forward. Published on August 29, 2016 as DOI: 10.1124/mol.116.105361
This article has not been copyedited and formatted. The final version may differ from this version.

ligands, KYN and XA, leading to chronically active AHR (Visual Abstract). AHR ligand concentrations within malignant cells and in the supernatant are sufficient to drive this amplification loop. At least one biological outcome of this chronic AHR stimulation is increased cell migration, a characteristic of aggressive, metastatic cells. Regulation of the kynurenine pathway by the AHR also has implications for tumor immunity, which is suppressed by the local production of kynurenine pathway metabolites. Finally, the data strongly suggest that targeting the kynurenine pathway, as in recent cancer therapy trials (Muller et al., 2005; Platten et al., 2014), and the AHR, may be effective approaches to $ER^-/PR^-/Her2^-$ breast cancer treatment. AHR inhibition may have the additional advantage of blocking AHR-driven tumor cell migration regardless of the nature of the endogenous AHR ligands. Since TDO over-expression has been reported for a wide range of cancers (Opitz et al., 2011; Pilotte et al., 2012), environmental and therapeutic implications of our findings may be generalizable to other malignancies.

Acknowledgements

The authors would like to acknowledge Dr. M. Pollastri for synthesizing FICZ and CH223191, Dr. M. Denison for his gift of the *pGudLuc* vector, Dr. S. Ethier for the SUM149 cells, Dr. Gabri van der Pluijm (Leiden University Medical Center) for the gift of MDA-MB-231-BO cells, Tufts University LC/MS Core Facility (NSF Awards 0821381 and 1337760) and the Boston University RT-PCR Core Facility for their assistance.

Molecular Pharmacology Fast Forward. Published on August 29, 2016 as DOI: 10.1124/mol.116.105361
This article has not been copyedited and formatted. The final version may differ from this version.

Author contributions

Participated in research design: Novikov, Sherr

Conducted experiments: Novikov, Wang, Parks, Ramirez-Cardenas, Stanford

Contributed new reagents or analytic tools: Lee, Manteiga, Monti, Li, Gusenleitner

Performed data analysis: Novikov, Sherr, Monti, Li, Gusenleitner, Landesman, Sarita-Reyes, Laklouk

Wrote or contributed to the writing of the manuscript: Novikov, Sherr, Wang, Parks, Ramirez-Cardenas, Stanford, Lee, Manteiga, Monti, Li, Gusenleitner, Landesman, Sarita-Reyes, Laklouk.

References

(2010) BioNumbers, Israel.

Abbott BD, Schmid JE, Pitt JA, Buckalew AR, Wood CR, Held GA and Diliberto JJ (1999) Adverse reproductive outcomes in the transgenic Ah receptor-deficient mouse. *Toxicology and applied pharmacology* **155**(1): 62-70.

Andersson P, McGuire J, Rubio C, Gradin K, Whitelaw ML, Pettersson S, Hanberg A and Poellinger L (2002) A constitutively active dioxin/aryl hydrocarbon receptor induces stomach tumors. *Proceedings of the National Academy of Sciences of the United States of America* **99**(15): 9990-9995.

Andreola F, Fernandez-Salguero PM, Chiantore MV, Petkovich MP, Gonzalez FJ and De Luca LM (1997) Aryl hydrocarbon receptor knockout mice (AHR-/-) exhibit liver retinoid accumulation and reduced retinoic acid metabolism. *Cancer research* **57**(14): 2835-2838.

Apetoh L, Quintana FJ, Pot C, Joller N, Xiao S, Kumar D, Burns EJ, Sherr DH, Weiner HL and Kuchroo VK (2010) The aryl hydrocarbon receptor interacts with c-Maf to promote the differentiation of type 1 regulatory T cells induced by IL-27. *Nature immunology* **11**(9): 854-861.

Bajad SU, Lu W, Kimball EH, Yuan J, Peterson C and Rabinowitz JD (2006) Separation and quantitation of water soluble cellular metabolites by hydrophilic interaction chromatography-tandem mass spectrometry. *Journal of chromatography A* **1125**(1): 76-88.

Barhoover MA, Hall JM, Greenlee WF and Thomas RS (2010) Aryl hydrocarbon receptor regulates cell cycle progression in human breast cancer cells via a functional interaction with cyclin-dependent kinase 4. *Molecular pharmacology* **77**(2): 195-201.

Barnett KR, Tomic D, Gupta RK, Babus JK, Roby KF, Terranova PF and Flaws JA (2007) The aryl hydrocarbon receptor is required for normal gonadotropin responsiveness in the mouse ovary. *Toxicology and applied pharmacology* **223**(1): 66-72.

Barouki R, Coumoul X and Fernandez-Salguero PM (2007) The aryl hydrocarbon receptor, more than a xenobiotic-interacting protein. *FEBS letters* **581**(19): 3608-3615.

Barretina J, Caponigro G, Stransky N, Venkatesan K, Margolin AA, Kim S, Wilson CJ, Lehar J, Kryukov GV, Sonkin D, Reddy A, Liu M, Murray L, Berger MF, Monahan JE, Morais P, Meltzer J, Korejwa A,

Jane-Valbuena J, Mapa FA, Thibault J, Bric-Furlong E, Raman P, Shipway A, Engels IH, Cheng J, Yu GK, Yu J, Aspesi P, Jr., de Silva M, Jagtap K, Jones MD, Wang L, Hatton C, Palescandolo E, Gupta S, Mahan S, Sougnez C, Onofrio RC, Liefeld T, MacConaill L, Winckler W, Reich M, Li N, Mesirov JP, Gabriel SB, Getz G, Ardlie K, Chan V, Myer VE, Weber BL, Porter J, Warmuth M, Finan P, Harris JL, Meyerson M, Golub TR, Morrissey MP, Sellers WR, Schlegel R and Garraway LA (2012) The Cancer Cell Line Encyclopedia enables predictive modelling of anticancer drug sensitivity. *Nature* **483**(7391): 603-607.

Belguise K, Guo S, Yang S, Rogers AE, Seldin DC, Sherr DH and Sonenshein GE (2007) Green tea polyphenols reverse cooperation between c-Rel and CK2 that induces the aryl hydrocarbon receptor, slug, and an invasive phenotype. *Cancer research* **67**(24): 11742-11750.

Bell ED, Bulbrook RD, Hayward JL and Tong D (1975) Tryptophan metabolism and recurrence rates of patients with breast cancer after mastectomy. *Acta vitaminologica et enzymologica* **29**(1-6): 104-107.

Bell EM, Mainwaring WI, Bulbrook RD, Tong D and Hayward JL (1971) Relationships between excretion of steroid hormones and tryptophan metabolites in patients with breast cancer. *The American journal of clinical nutrition* **24**(6): 694-698.

Benedict JC, Lin TM, Loeffler IK, Peterson RE and Flaws JA (2000) Physiological role of the aryl hydrocarbon receptor in mouse ovary development. *Toxicological sciences : an official journal of the Society of Toxicology* **56**(2): 382-388.

Brandacher G, Perathoner A, Ladurner R, Schneeberger S, Obrist P, Winkler C, Werner ER, Werner-Felmayer G, Weiss HG, Gobel G, Margreiter R, Konigsrainer A, Fuchs D and Amberger A (2006) Prognostic value of indoleamine 2,3-dioxygenase expression in colorectal cancer: effect on tumor-infiltrating T cells. *Clinical cancer research : an official journal of the American Association for Cancer Research* **12**(4): 1144-1151.

Braun D, Longman RS and Albert ML (2005) A two-step induction of indoleamine 2,3 dioxygenase (IDO) activity during dendritic-cell maturation. *Blood* **106**(7): 2375-2381.

Brody JG, Moysich KB, Humblet O, Attfield KR, Beehler GP and Rudel RA (2007) Environmental pollutants and breast cancer: epidemiologic studies. *Cancer* **109**(12 Suppl): 2667-2711.

Brooks J and Eltom SE (2011) Malignant transformation of mammary epithelial cells by ectopic overexpression of the aryl hydrocarbon receptor. *Current cancer drug targets* **11**(5): 654-669.

Bunger MK, Moran SM, Glover E, Thomae TL, Lahvis GP, Lin BC and Bradfield CA (2003) Resistance to 2,3,7,8-tetrachlorodibenzo-p-dioxin toxicity and abnormal liver development in mice carrying a mutation in the nuclear localization sequence of the aryl hydrocarbon receptor. *The Journal of biological chemistry* **278**(20): 17767-17774.

Calaf G and Russo J (1993) Transformation of human breast epithelial cells by chemical carcinogens. *Carcinogenesis* **14**(3): 483-492.

Cancer Genome Atlas N (2012) Comprehensive molecular portraits of human breast tumours. *Nature* **490**(7418): 61-70.

Casado FL, Singh KP and Gasiewicz TA (2011) Aryl hydrocarbon receptor activation in hematopoietic stem/progenitor cells alters cell function and pathway-specific gene modulation reflecting changes in cellular trafficking and migration. *Molecular pharmacology* **80**(4): 673-682.

Cascino A, Cangiano C, Ceci F, Franchi F, Mineo T, Mulieri M, Muscaritoli M and Rossi Fanelli F (1991) Increased plasma free tryptophan levels in human cancer: a tumor related effect? *Anticancer research* **11**(3): 1313-1316.

Cascino A, Muscaritoli M, Cangiano C, Conversano L, Laviano A, Ariemma S, Meguid MM and Rossi Fanelli F (1995) Plasma amino acid imbalance in patients with lung and breast cancer. *Anticancer research* **15**(2): 507-510.

Chang CY and Puga A (1998) Constitutive activation of the aromatic hydrocarbon receptor. *Molecular and cellular biology* **18**(1): 525-535.

Chang JT, Chang H, Chen PH, Lin SL and Lin P (2007) Requirement of aryl hydrocarbon receptor overexpression for CYP1B1 up-regulation and cell growth in human lung adenocarcinomas. *Clinical cancer research : an official journal of the American Association for Cancer Research* **13**(1): 38-45.

Chen JY, Li CF, Kuo CC, Tsai KK, Hou MF and Hung WC (2014) Cancer/stroma interplay via cyclooxygenase-2 and indoleamine 2,3-dioxygenase promotes breast cancer progression. *Breast cancer research : BCR* **16**(4): 410.

Chen Y and Guillemin GJ (2009) Kynurenine pathway metabolites in humans: disease and healthy States. *International journal of tryptophan research : IJTR* **2**: 1-19.

Chen Y, Zhang R, Song Y, He J, Sun J, Bai J, An Z, Dong L, Zhan Q and Abliz Z (2009) RRLC-MS/MS-based metabonomics combined with in-depth analysis of metabolic correlation network: finding potential biomarkers for breast cancer. *The Analyst* **134**(10): 2003-2011.

Chevolet I, Speeckaert R, Haspeslagh M, Neyns B, Kruse V, Schreuer M, Van Gele M, Van Geel N and Brochez L (2014) Peritumoral indoleamine 2,3-dioxygenase expression in melanoma: an early marker of resistance to immune control? *The British journal of dermatology* **171**(5): 987-995.

Choe JY, Yun JY, Jeon YK, Kim SH, Park G, Huh JR, Oh S and Kim JE (2014) Indoleamine 2,3-dioxygenase (IDO) is frequently expressed in stromal cells of Hodgkin lymphoma and is associated with adverse clinical features: a retrospective cohort study. *BMC cancer* **14**: 335.

Chung KT and Gadupudi GS (2011) Possible roles of excess tryptophan metabolites in cancer. *Environmental and molecular mutagenesis* **52**(2): 81-104.

Currier N, Solomon SE, Demicco EG, Chang DL, Farago M, Ying H, Dominguez I, Sonenshein GE, Cardiff RD, Xiao ZX, Sherr DH and Seldin DC (2005) Oncogenic signaling pathways activated in DMBA-induced mouse mammary tumors. *Toxicologic pathology* **33**(6): 726-737.

D'Amato NC, Rogers TJ, Gordon MA, Greene LI, Cochrane DR, Spoelstra NS, Nemkov TG, D'Alessandro A, Hansen KC and Richer JK (2015) A TDO2-AhR Signaling Axis Facilitates Anoikis Resistance and Metastasis in Triple-Negative Breast Cancer. *Cancer research* **75**(21): 4651-4664.

Dai M, Wang P, Boyd AD, Kostov G, Athey B, Jones EG, Bunney WE, Myers RM, Speed TP, Akil H, Watson SJ and Meng F (2005) Evolving gene/transcript definitions significantly alter the interpretation of GeneChip data. *Nucleic acids research* **33**(20): e175.

Davis HL, Jr., Brown RR, Leklem J and Carlson IH (1973) Tryptophan metabolism in breast cancer. Correlation with urinary steroid excretion. *Cancer* **31**(5): 1061-1064.

DeGeorge FV and Brown RR (1970) Differences in tryptophan metabolism between breast cancer patients with and without cancer at other sites. *Cancer* **26**(4): 767-770.

Dietrich C and Kaina B (2010) The aryl hydrocarbon receptor (AhR) in the regulation of cell-cell contact and tumor growth. *Carcinogenesis* **31**(8): 1319-1328.

DiNatale BC, Murray IA, Schroeder JC, Flaveny CA, Lahoti TS, Laurenzana EM, Omiecinski CJ and Perdew GH (2010) Kynurenic acid is a potent endogenous aryl hydrocarbon receptor ligand that synergistically induces interleukin-6 in the presence of inflammatory signaling. *Toxicological sciences : an official journal of the Society of Toxicology* **115**(1): 89-97.

DiNatale BC, Schroeder JC and Perdew GH (2011) Ah receptor antagonism inhibits constitutive and cytokine inducible IL6 production in head and neck tumor cell lines. *Molecular carcinogenesis* **50**(3): 173-183.

DiNatale BC, Smith K, John K, Krishnegowda G, Amin SG and Perdew GH (2012) Ah receptor antagonism represses head and neck tumor cell aggressive phenotype. *Molecular cancer research : MCR* **10**(10): 1369-1379.

Diry M, Tomkiewicz C, Koehle C, Coumoul X, Bock KW, Barouki R and Transy C (2006) Activation of the dioxin/aryl hydrocarbon receptor (AhR) modulates cell plasticity through a JNK-dependent mechanism. *Oncogene* **25**(40): 5570-5574.

Do MT, Kim HG, Tran TT, Khanal T, Choi JH, Chung YC, Jeong TC and Jeong HG (2014) Metformin suppresses CYP1A1 and CYP1B1 expression in breast cancer cells by down-regulating aryl hydrocarbon receptor expression. *Toxicology and applied pharmacology* **280**(1): 138-148.

Ema M, Ohe N, Suzuki M, Mimura J, Sogawa K, Ikawa S and Fujii-Kuriyama Y (1994) Dioxin binding activities of polymorphic forms of mouse and human arylhydrocarbon receptors. *The Journal of biological chemistry* **269**(44): 27337-27343.

Endler A, Chen L and Shibasaki F (2014) Coactivator recruitment of AhR/ARNT1. *International journal of molecular sciences* **15**(6): 11100-11110.

Fahl WE, Rose DP, Liskowski L and Brown RR (1974) Tryptophan metabolism and corticosteroids in breast cancer. *Cancer* **34**(5): 1691-1695.

Fernadez-Saluero PM, Ward JM, Sundberg JP and Gonzalez FJ (1997) Lesions of aryl-hydrocarbon receptor-deficient mice. *Vet Pathol* **34**: 605-614.

Fernandez-Salguero P, Pineau T, Hilbert DM, McPhail T, Lee SS, Kimura S, Nebert DW, Rudikoff S, Ward JM and Gonzalez FJ (1995) Immune system impairment and hepatic fibrosis in mice lacking the dioxin-binding Ah receptor. *Science* **268**(5211): 722-726.

Funatake CJ, Marshall NB, Steppan LB, Mourich DV and Kerkvliet NI (2005) Cutting edge: activation of the aryl hydrocarbon receptor by 2,3,7,8-tetrachlorodibenzo-p-dioxin generates a population of CD4+ CD25+ cells with characteristics of regulatory T cells. *Journal of immunology* **175**(7): 4184-4188.

Gagliani N, Vesely MC, Iseppon A, Brockmann L, Xu H, Palm NW, de Zoete MR, Licona-Limon P, Paiva RS, Ching T, Weaver C, Zi X, Pan X, Fan R, Garmire LX, Cotton MJ, Drier Y, Bernstein B, Geginat J, Stockinger B, Esplugues E, Huber S and Flavell RA (2015) Th17 cells transdifferentiate into regulatory T cells during resolution of inflammation. *Nature* **523**(7559): 221-225.

Garrett RW and Gasiewicz TA (2006) The aryl hydrocarbon receptor agonist 2,3,7,8-tetrachlorodibenzo-p-dioxin alters the circadian rhythms, quiescence, and expression of clock genes in murine hematopoietic stem and progenitor cells. *Molecular pharmacology* **69**(6): 2076-2083.

Girgin G, Tolga Sahin T, Fuchs D, Kasuya H, Yuksel O, Tekin E and Baydar T (2009) Immune system modulation in patients with malignant and benign breast disorders: tryptophan degradation and serum neopterin. *The International journal of biological markers* **24**(4): 265-270.

Goode G, Pratap S and Eltom SE (2014) Depletion of the aryl hydrocarbon receptor in MDA-MB-231 human breast cancer cells altered the expression of genes in key regulatory pathways of cancer. *PloS one* **9**(6): e100103.

Goode GD, Ballard BR, Manning HC, Freeman ML, Kang Y and Eltom SE (2013) Knockdown of aberrantly upregulated aryl hydrocarbon receptor reduces tumor growth and metastasis of MDA-MB-231 human breast cancer cell line. *International journal of cancer Journal international du cancer* **133**(12): 2769-2780.

Gramatzki D, Pantazis G, Schittenhelm J, Tabatabai G, Kohle C, Wick W, Schwarz M, Weller M and Tritschler I (2009) Aryl hydrocarbon receptor inhibition downregulates the TGF-beta/Smad pathway in human glioblastoma cells. *Oncogene* **28**(28): 2593-2605.

Hahn ME (1998) The aryl hydrocarbon receptor: a comparative perspective. *Comparative biochemistry and physiology Part C, Pharmacology, toxicology & endocrinology* **121**(1-3): 23-53.

Hahn ME (2002) Aryl hydrocarbon receptors: diversity and evolution. *Chemico-biological interactions* **141**(1-2): 131-160.

Hall JM, Barhoover MA, Kazmin D, McDonnell DP, Greenlee WF and Thomas RS (2010) Activation of the aryl-hydrocarbon receptor inhibits invasive and metastatic features of human breast cancer cells and promotes breast cancer cell differentiation. *Molecular endocrinology* **24**(2): 359-369.

Hara T, Yamakura F, Takikawa O, Hiramatsu R, Kawabe T, Isobe K and Nagase F (2008) Diazotization of kynurenine by acidified nitrite secreted from indoleamine 2,3-dioxygenase-expressing myeloid dendritic cells. *Journal of immunological methods* **332**(1-2): 162-169.

Hayashibara T, Yamada Y, Mori N, Harasawa H, Sugahara K, Miyanishi T, Kamihira S and Tomonaga M (2003) Possible involvement of aryl hydrocarbon receptor (AhR) in adult T-cell leukemia (ATL) leukemogenesis: constitutive activation of AhR in ATL. *Biochemical and biophysical research communications* **300**(1): 128-134.

Heath-Pagliuso S, Rogers WJ, Tullis K, Seidel SD, Cenijn PH, Brouwer A and Denison MS (1998) Activation of the Ah receptor by tryptophan and tryptophan metabolites. *Biochemistry* **37**(33): 11508-11515.

Hester I, McKee S, Pelletier P, Thompson C, Storbeck C, Mears A, Schulz JB, Hakim AA and Sabourin LA (2007) Transient expression of Nxf, a bHLH-PAS transactivator induced by neuronal preconditioning, confers neuroprotection in cultured cells. *Brain research* **1135**(1): 1-11.

Hirota K (2015) Involvement of hypoxia-inducible factors in the dysregulation of oxygen homeostasis in sepsis. *Cardiovascular & hematological disorders drug targets* **15**(1): 29-40.

Huang X, Powell-Coffman JA and Jin Y (2004) The AHR-1 aryl hydrocarbon receptor and its co-factor the AHA-1 aryl hydrocarbon receptor nuclear translocator specify GABAergic neuron cell fate in C. elegans. *Development* **131**(4): 819-828.

Hwang SL, Chung NP, Chan JK and Lin CL (2005) Indoleamine 2, 3-dioxygenase (IDO) is essential for dendritic cell activation and chemotactic responsiveness to chemokines. *Cell research* **15**(3): 167-175.

Ichihara S, Yamada Y, Ichihara G, Nakajima T, Li P, Kondo T, Gonzalez FJ and Murohara T (2007) A role for the aryl hydrocarbon receptor in regulation of ischemia-induced angiogenesis. *Arterioscler Thromb Vasc Biol* **27**(6): 1297-1304.

Irizarry RA, Hobbs B, Collin F, Beazer-Barclay YD, Antonellis KJ, Scherf U and Speed TP (2003) Exploration, normalization, and summaries of high density oligonucleotide array probe level data. *Biostatistics* **4**(2): 249-264.

Jensen KA, Luu TC and Chan WK (2006) A truncated Ah receptor blocks the hypoxia and estrogen receptor signaling pathways: a viable approach for breast cancer treatment. *Mol Pharm* **3**(6): 695-703.

Jin UH, Kim SB and Safe S (2015) Omeprazole Inhibits Pancreatic Cancer Cell Invasion through a Nongenomic Aryl Hydrocarbon Receptor Pathway. *Chemical research in toxicology* **28**(5): 907-918.

Jin UH, Lee SO, Pfent C and Safe S (2014) The aryl hydrocarbon receptor ligand omeprazole inhibits breast cancer cell invasion and metastasis. *BMC cancer* **14**: 498.

Kerkvliet NI (2009) AHR-mediated immunomodulation: the role of altered gene transcription. *Biochemical pharmacology* **77**(4): 746-760.

Kim DW, Gazourian L, Quadri SA, Romieu-Mourez R, Sherr DH and Sonenshein GE (2000) The RelA NF-kappaB subunit and the aryl hydrocarbon receptor (AhR) cooperate to transactivate the c-myc promoter in mammary cells. *Oncogene* **19**(48): 5498-5506.

Kimura A, Naka T, Nakahama T, Chinen I, Masuda K, Nohara K, Fujii-Kuriyama Y and Kishimoto T (2009) Aryl hydrocarbon receptor in combination with Stat1 regulates LPS-induced inflammatory responses. *The Journal of experimental medicine* **206**(9): 2027-2035.

Koliopanos A, Kleeff J, Xiao Y, Safe S, Zimmermann A, Buchler MW and Friess H (2002) Increased arylhydrocarbon receptor expression offers a potential therapeutic target for pancreatic cancer. *Oncogene* **21**(39): 6059-6070.

Korzeniewski N, Wheeler S, Chatterjee P, Duensing A and Duensing S (2010) A novel role of the aryl hydrocarbon receptor (AhR) in centrosome amplification - implications for chemoprevention. *Molecular cancer* **9**: 153.

Lahoti TS, Hughes JM, Kusnadi A, John K, Zhu B, Murray IA, Gowda K, Peters JM, Amin SG and Perdew GH (2014) Aryl hydrocarbon receptor antagonism attenuates growth factor expression, proliferation, and migration in fibroblast-like synoviocytes from patients with rheumatoid arthritis. *The Journal of pharmacology and experimental therapeutics* **348**(2): 236-245.

Lahvis GP, Lindell SL, Thomas RS, McCuskey RS, Murphy C, Glover E, Bentz M, Southard J and Bradfield CA (2000) Portosystemic shunting and persistent fetal vascular structures in aryl hydrocarbon receptor-deficient mice. *Proceedings of the National Academy of Sciences of the United States of America* **97**(19): 10442-10447.

Lahvis GP, Pyzalski RW, Glover E, Pitot HC, McElwee MK and Bradfield CA (2005) The aryl hydrocarbon receptor is required for developmental closure of the ductus venosus in the neonatal mouse. *Molecular pharmacology* **67**(3): 714-720.

Larsen MC, Brake PB, Pollenz RS and Jefcoate CR (2004) Linked expression of Ah receptor, ARNT, CYP1A1, and CYP1B1 in rat mammary epithelia, in vitro, is each substantially elevated by specific extracellular matrix interactions that precede branching morphogenesis. *Toxicological sciences : an official journal of the Society of Toxicology* **82**(1): 46-61.

Lee YK, Lee HB, Shin DM, Kang MJ, Yi EC, Noh S, Lee J, Lee C, Min CK and Choi EY (2014) Heme-binding-mediated negative regulation of the tryptophan metabolic enzyme indoleamine 2,3-dioxygenase 1 (IDO1) by IDO2. *Experimental & molecular medicine* **46**: e121.

Lehrer S, Brown RR, Lee CM, Song HK, Kalnicki S, Lipsztein R, Dalton J and Bloomer WD (1988) Tryptophan metabolism in women with breast cancer. *International journal of cancer Journal international du cancer* **42**(1): 137.

Li B and Dewey CN (2011) RSEM: accurate transcript quantification from RNA-Seq data with or without a reference genome. *BMC bioinformatics* **12**: 323.

Li D, Zhang W, Sahin AA and Hittelman WN (1999) DNA adducts in normal tissue adjacent to breast cancer: a review. *Cancer Detect Prev* **23**(6): 454-462.

Li ZD, Wang K, Yang XW, Zhuang ZG, Wang JJ and Tong XW (2014) Expression of aryl hydrocarbon receptor in relation to p53 status and clinicopathological parameters in breast cancer. *International journal of clinical and experimental pathology* **7**(11): 7931-7937.

Liu Z, Wu X, Zhang F, Han L, Bao G, He X and Xu Z (2013) AhR expression is increased in hepatocellular carcinoma. *Journal of molecular histology* **44**(4): 455-461.

Lyon DE, Walter JM, Starkweather AR, Schubert CM and McCain NL (2011) Tryptophan degradation in women with breast cancer: a pilot study. *BMC research notes* **4**: 156.

Manuwald U, Velasco Garrido M, Berger J, Manz A and Baur X (2012) Mortality study of chemical workers exposed to dioxins: follow-up 23 years after chemical plant closure. *Occupational and environmental medicine* **69**(9): 636-642.

McGregor DB1 PC, Wilbourn J, Rice JM. (1998) An IARC evaluation of polychlorinated dibenzo-p-dioxins and polychlorinated dibenzofurans as risk factors in human carcinogenesis. *Environ Health Perspect* **106**(Suppl 2): 755-760.

Mellor AL and Munn DH (2004) IDO expression by dendritic cells: tolerance and tryptophan catabolism. *Nature reviews Immunology* **4**(10): 762-774.

Mezrich JD, Fechner JH, Zhang X, Johnson BP, Burlingham WJ and Bradfield CA (2010) An interaction between kynurenine and the aryl hydrocarbon receptor can generate regulatory T cells. *Journal of immunology* **185**(6): 3190-3198.

Milo R, Jorgensen P, Moran U, Weber G and Springer M (2010) BioNumbers--the database of key numbers in molecular and cell biology. *Nucleic acids research* **38**(Database issue): D750-753.

Muller AJ, Malachowski WP and Prendergast GC (2005) Indoleamine 2,3-dioxygenase in cancer: targeting pathological immune tolerance with small-molecule inhibitors. *Expert opinion on therapeutic targets* **9**(4): 831-849.

Murray IA, Patterson AD and Perdew GH (2014) Aryl hydrocarbon receptor ligands in cancer: friend and foe. *Nature reviews Cancer* **14**(12): 801-814.

Nguyen NT, Kimura A, Nakahama T, Chinen I, Masuda K, Nohara K, Fujii-Kuriyama Y and Kishimoto T (2010) Aryl hydrocarbon receptor negatively regulates dendritic cell immunogenicity via a kynurenine-dependent mechanism. *Proceedings of the National Academy of Sciences of the United States of America* **107**(46): 19961-19966.

Opitz CA, Litzenburger UM, Sahm F, Ott M, Tritschler I, Trump S, Schumacher T, Jestaedt L, Schrenk D, Weller M, Jugold M, Guillemin GJ, Miller CL, Lutz C, Radlwimmer B, Lehmann I, von Deimling A, Wick W and Platten M (2011) An endogenous tumour-promoting ligand of the human aryl hydrocarbon receptor. *Nature* **478**(7368): 197-203.

Parks AJ, Pollastri MP, Hahn ME, Stanford EA, Novikov O, Franks DG, Haigh SE, Narasimhan S, Ashton TD, Hopper TG, Kozakov D, Beglov D, Vajda S, Schlezinger JJ and Sherr DH (2014) In silico

identification of an aryl hydrocarbon receptor antagonist with biological activity in vitro and in vivo. *Molecular pharmacology* **86**(5): 593-608.

Pfaffl MW (2001) A new mathematical model for relative quantification in real-time RT-PCR. *Nucleic acids research* **29**(9): e45.

Pilotte L, Larrieu P, Stroobant V, Colau D, Dolusic E, Frederick R, De Plaen E, Uyttenhove C, Wouters J, Masereel B and Van den Eynde BJ (2012) Reversal of tumoral immune resistance by inhibition of tryptophan 2,3-dioxygenase. *Proceedings of the National Academy of Sciences of the United States of America* **109**(7): 2497-2502.

Platten M, von Knebel Doeberitz N, Oezen I, Wick W and Ochs K (2014) Cancer Immunotherapy by Targeting IDO1/TDO and Their Downstream Effectors. *Frontiers in immunology* **5**: 673.

Prud'homme GJ, Glinka Y, Toulina A, Ace O, Subramaniam V and Jothy S (2010) Breast cancer stem-like cells are inhibited by a non-toxic aryl hydrocarbon receptor agonist. *PloS one* **5**(11): e13831.

Puccetti P, Fallarino F, Italiano A, Soubeyran I, MacGrogan G, Debled M, Velasco V, Bodet D, Eimer S, Veldhoen M, Prendergast GC, Platten M, Bessede A and Guillemin GJ (2015) Accumulation of an endogenous tryptophan-derived metabolite in colorectal and breast cancers. *PloS one* **10**(4): e0122046.

Quintana FJ, Basso AS, Iglesias AH, Korn T, Farez MF, Bettelli E, Caccamo M, Oukka M and Weiner HL (2008) Control of T(reg) and T(H)17 cell differentiation by the aryl hydrocarbon receptor. *Nature* **453**(7191): 65-71.

Revich B, Aksel E, Ushakova T, Ivanova I, Zhuchenko N, Klyuev N, Brodsky B and Sotskov Y (2001) Dioxin exposure and public health in Chapaevsk, Russia. *Chemosphere* **43**(4-7): 951-966.

Roblin S, Okey AB and Harper PA (2004) AH receptor antagonist inhibits constitutive CYP1A1 and CYP1B1 expression in rat BP8 cells. *Biochemical and biophysical research communications* **317**(1): 142-148.

Russo J, Calaf G and Russo IH (1993) A critical approach to the malignant transformation of human breast epithelial cells with chemical carcinogens. *Critical reviews in oncogenesis* **4**(4): 403-417.

Safe S, Lee SO and Jin UH (2013) Role of the aryl hydrocarbon receptor in carcinogenesis and potential as a drug target. *Toxicological sciences : an official journal of the Society of Toxicology* **135**(1): 1-16.

Sakurai K, Amano S, Enomoto K, Kashio M, Saito Y, Sakamoto A, Matsuo S, Suzuki M, Kitajima A, Hirano T and Negishi N (2005) [Study of indoleamine 2,3-dioxygenase expression in patients with breast cancer]. *Gan To Kagaku Ryoho* **32**(11): 1546-1549.

Sanjana NE, Shalem O and Zhang F (2014) Improved vectors and genome-wide libraries for CRISPR screening. *Nature methods* **11**(8): 783-784.

Schlezinger JJ, Liu D, Farago M, Seldin DC, Belguise K, Sonenshein GE and Sherr DH (2006) A role for the aryl hydrocarbon receptor in mammary gland tumorigenesis. *Biological chemistry* **387**(9): 1175-1187.

Schmidt J, Su G, Simon JRM and Bradfield C (1996) Characterization of a murine *Ahr* null allele: Involvement of the Ah receptor in hepatic growth and development. *Proc Natl Acad Sci USA* **93**: 6731-6736.

Schroeder JC, Dinatale BC, Murray IA, Flaveny CA, Liu Q, Laurenzana EM, Lin JM, Strom SC, Omiecinski CJ, Amin S and Perdew GH The uremic toxin 3-indoxyl sulfate is a potent endogenous agonist for the human aryl hydrocarbon receptor. *Biochemistry* **49**(2): 393-400.

Sherr DH and Monti S (2013) The role of the aryl hydrocarbon receptor in normal and malignant B cell development. *Seminars in immunopathology* **35**(6): 705-716.

Shivanna S, Kolandaivelu K, Shashar M, Belghasim M, Al-Rabadi L, Balcells M, Zhang A, Weinberg J, Francis J, Pollastri MP, Edelman ER, Sherr DH and Chitalia VC (2016) The Aryl Hydrocarbon Receptor is a Critical Regulator of Tissue Factor Stability and an Antithrombotic Target in Uremia. *Journal of the American Society of Nephrology : JASN* **27**(1): 189-201.

Smith BW, Rozelle SS, Leung A, Ubellacker J, Parks A, Nah SK, French D, Gadue P, Monti S, Chui DH, Steinberg MH, Frelinger AL, Michelson AD, Theberge R, McComb ME, Costello CE, Kotton DN, Mostoslavsky G, Sherr DH and Murphy GJ (2013) The aryl hydrocarbon receptor directs hematopoietic progenitor cell expansion and differentiation. *Blood* **122**(3): 376-385.

Smith C, Chang MY, Parker KH, Beury DW, DuHadaway JB, Flick HE, Boulden J, Sutanto-Ward E, Soler AP, Laury-Kleintop LD, Mandik-Nayak L, Metz R, Ostrand-Rosenberg S, Prendergast GC and Muller AJ (2012) IDO is a nodal pathogenic driver of lung cancer and metastasis development. *Cancer discovery* **2**(8): 722-735.

Soichot M, Vaast A, Vignau J, Guillemin GJ, Lhermitte M, Broly F and Allorge D (2013) Characterization of functional polymorphisms and glucocorticoid-responsive elements in the promoter of TDO2, a candidate gene for ethanol-induced behavioural disorders. *Alcohol and alcoholism* **48**(4): 415-425.

Stanford EA, Ramirez-Cardenas A, Wang Z, Novikov O, Alamoud K, Koutrakis P, Mizgerd JP, Genco CA, Kukuruzinska M, Monti S, Bais MV and Sherr DH (2016a) Role for the Aryl Hydrocarbon Receptor and Diverse Ligands In Oral Squamous Cell Carcinoma Migration and Tumorigenesis. *Molecular cancer research : MCR*.

Stanford EA, Wang Z, Novikov O, Mulas F, Landesman-Bollag E, Monti S, Smith BW, Seldin DC, Murphy GJ and Sherr DH (2016b) The role of the aryl hydrocarbon receptor in the development of cells with the molecular and functional characteristics of cancer stem-like cells. *BMC biology* **14**(1): 20.

Staudacher A, Hinz T, Novak N, von Bubnoff D and Bieber T (2015) Exaggerated IDO1 expression and activity in Langerhans cells from patients with atopic dermatitis upon viral stimulation: a potential predictive biomarker for high risk of Eczema herpeticum. *Allergy* **70**(11): 1432-1439.

Tang X, Lin CC, Spasojevic I, Iversen ES, Chi JT and Marks JR (2014) A joint analysis of metabolomics and genetics of breast cancer. *Breast cancer research : BCR* **16**(4): 415.

Team RC (2012) R: A Language and Environment for Statistical Computing.

Thackaberry EA, Gabaldon DM, Walker MK and Smith SM (2002) Aryl hydrocarbon receptor null mice develop cardiac hypertrophy and increased hypoxia-inducible factor-1alpha in the absence of cardiac hypoxia. *Cardiovascular toxicology* **2**(4): 263-274.

Theate I, van Baren N, Pilotte L, Moulin P, Larrieu P, Renauld JC, Herve C, Gutierrez-Roelens I, Marbaix E, Sempoux C and Van den Eynde BJ (2015) Extensive profiling of the expression of the indoleamine 2,3-dioxygenase 1 protein in normal and tumoral human tissues. *Cancer immunology research* **3**(2): 161-172.

Travers MT, Gow IF, Barber MC, Thomson J and Shennan DB (2004) Indoleamine 2,3-dioxygenase activity and L-tryptophan transport in human breast cancer cells. *Biochimica et biophysica acta* **1661**(1): 106-112.

Trombino AF, Near RI, Matulka RA, Yang S, Hafer LJ, Toselli PA, Kim DW, Rogers AE, Sonenshein GE and Sherr DH (2000) Expression of the aryl hydrocarbon receptor/transcription factor (AhR) and

AhR-regulated CYP1 gene transcripts in a rat model of mammary tumorigenesis. *Breast cancer research and treatment* **63**(2): 117-131.

Uyttenhove C, Pilotte L, Theate I, Stroobant V, Colau D, Parmentier N, Boon T and Van den Eynde BJ (2003) Evidence for a tumoral immune resistance mechanism based on tryptophan degradation by indoleamine 2,3-dioxygenase. *Nature medicine* **9**(10): 1269-1274.

van Baren N and Van den Eynde BJ (2015) Tryptophan-degrading enzymes in tumoral immune resistance. *Frontiers in immunology* **6**: 34.

van Zijl F, Krupitza G and Mikulits W (2011) Initial steps of metastasis: cell invasion and endothelial transmigration. *Mutation research* **728**(1-2): 23-34.

Vasquez A, Atallah-Yunes N, Smith FC, You X, Chase SE, Silverstone AE and Vikstrom KL (2003) A role for the aryl hydrocarbon receptor in cardiac physiology and function as demonstrated by AhR knockout mice. *Cardiovascular toxicology* **3**(2): 153-163.

Vogel CF, Goth SR, Dong B, Pessah IN and Matsumura F (2008) Aryl hydrocarbon receptor signaling mediates expression of indoleamine 2,3-dioxygenase. *Biochemical and biophysical research communications* **375**(3): 331-335.

Vogel CF, Li W, Wu D, Miller JK, Sweeney C, Lazennec G, Fujisawa Y and Matsumura F (2011) Interaction of aryl hydrocarbon receptor and NF-kappaB subunit RelB in breast cancer is associated with interleukin-8 overexpression. *Archives of biochemistry and biophysics* **512**(1): 78-86.

Wang F, Wang W and Safe S (1999) Regulation of constitutive gene expression through interactions of Sp1 protein with the nuclear aryl hydrocarbon receptor complex. *Biochemistry* **38**(35): 11490-11500.

Wang K, Li Y, Jiang YZ, Dai CF, Patankar MS, Song JS and Zheng J (2013a) An endogenous aryl hydrocarbon receptor ligand inhibits proliferation and migration of human ovarian cancer cells. *Cancer letters* **340**(1): 63-71.

Wang Q, Chen J, Ko CI, Fan Y, Carreira V, Chen Y, Xia Y, Medvedovic M and Puga A (2013b) Disruption of aryl hydrocarbon receptor homeostatic levels during embryonic stem cell differentiation alters expression of homeobox transcription factors that control cardiomyogenesis. *Environ Health Perspect* **121**(11-12): 1334-1343.

Warner M, Eskenazi B, Mocarelli P, Gerthoux PM, Samuels S, Needham L, Patterson D and Brambilla P (2002) Serum dioxin concentrations and breast cancer risk in the Seveso Women's Health Study. *Environ Health Perspect* **110**(7): 625-628.

Warner M, Mocarelli P, Samuels S, Needham L, Brambilla P and Eskenazi B (2011) Dioxin exposure and cancer risk in the Seveso Women's Health Study. *Environ Health Perspect* **119**(12): 1700-1705.

Wetterwald A, van der Pluijm G, Que I, Sijmons B, Buijs J, Karperien M, Lowik CW, Gautschi E, Thalmann GN and Cecchini MG (2002) Optical imaging of cancer metastasis to bone marrow: a mouse model of minimal residual disease. *The American journal of pathology* **160**(3): 1143-1153.

Xu CX, Krager SL, Liao DF and Tischkau SA (2010) Disruption of CLOCK-BMAL1 transcriptional activity is responsible for aryl hydrocarbon receptor-mediated regulation of Period1 gene. *Toxicological sciences : an official journal of the Society of Toxicology* **115**(1): 98-108.

Yang X, Liu D, Murray TJ, Mitchell GC, Hesterman EV, Karchner SI, Merson RR, Hahn ME and Sherr DH (2005) The aryl hydrocarbon receptor constitutively represses c-myc transcription in human mammary tumor cells. *Oncogene* **24**(53): 7869-7881.

Yang X, Solomon S, Fraser LR, Trombino AF, Liu D, Sonenshein GE, Hestermann EV and Sherr DH (2008) Constitutive regulation of CYP1B1 by the aryl hydrocarbon receptor (AhR) in pre-malignant and malignant mammary tissue. *Journal of cellular biochemistry* **104**(2): 402-417.

Yeung AW, Terentis AC, King NJ and Thomas SR (2015) Role of indoleamine 2,3-dioxygenase in health and disease. *Clinical science* **129**(7): 601-672.

Yoneda T, Williams PJ, Hiraga T, Niewolna M and Nishimura R (2001) A bone-seeking clone exhibits different biological properties from the MDA-MB-231 parental human breast cancer cells and a brain-seeking clone in vivo and in vitro. *Journal of bone and mineral research : the official journal of the American Society for Bone and Mineral Research* **16**(8): 1486-1495.

Yuan M, Breitkopf SB, Yang X and Asara JM (2012) A positive/negative ion-switching, targeted mass spectrometry-based metabolomics platform for bodily fluids, cells, and fresh and fixed tissue. *Nature protocols* **7**(5): 872-881.

Molecular Pharmacology Fast Forward. Published on August 29, 2016 as DOI: 10.1124/mol.116.105361
This article has not been copyedited and formatted. The final version may differ from this version.

Zhao S, Kanno Y, Nakayama M, Makimura M, Ohara S and Inouye Y (2012) Activation of the aryl hydrocarbon receptor represses mammosphere formation in MCF-7 cells. *Cancer letters* **317**(2): 192-198.

Zhao S, Ohara S, Kanno Y, Midorikawa Y, Nakayama M, Makimura M, Park Y and Inouye Y (2013) HER2 overexpression-mediated inflammatory signaling enhances mammosphere formation through up-regulation of aryl hydrocarbon receptor transcription. *Cancer letters* **330**(1): 41-48.

Molecular Pharmacology Fast Forward. Published on August 29, 2016 as DOI: 10.1124/mol.116.105361
This article has not been copyedited and formatted. The final version may differ from this version.

Footnotes:

This work was supported by National Institutes of Environmental Health Sciences [P42-ES007381, P42 ES007381S2]; The Art beCAUSE Breast Cancer Foundation; The Mary Kay Foundation; and the Avon Breast Cancer Foundation

Molecular Pharmacology Fast Forward. Published on August 29, 2016 as DOI: 10.1124/mol.116.105361
This article has not been copyedited and formatted. The final version may differ from this version.

Figure Legends:

Figure 1. Positive correlation between *AHR* and *CYP1B1* mRNA expression in breast cancer cell lines and primary breast cancers. Presented are linear regression analyses of *AHR* and *CYP1B1* expression using data from: **A)** Fifty-eight breast cancer cell lines in the Cancer Cell Line Encyclopedia (CCLE) database and **B)** 977 primary breast cancers in The Cancer Genome Atlas (TCGA). Pearson moment correlation coefficients (r) and false discovery rates (FDR) are reported for each correlation. Grey-filled circles represent ER^- negative cell lines (**A**) and primary cancers (**B**).

Figure 2. Immunohistochemistry of primary breast tumors and patient-matched lymph node metastasis demonstrating AHR and TDO expression. Tissue microarrays of ER^+ and $ER^-/PR^-/Her2^-$ invasive ductal carcinomas from 50 cases was analyzed by immunohistochemistry for AHR and TDO expression. Representative photos of an ER+ (left panels) and TNBC (right panels) primary tissue and matched lymph node (LN) metastasis are shown. Red arrows indicate nuclear AHR localization.

Figure 3. *TDO2* expression is elevated in primary breast tumors. *TDO2* expression data for primary breast tumors (T) and paired histologically normal "adjacent normal" tissue (AN) were acquired from the cancer genome atlas (TCGA) and plotted with respect to: **A)** estrogen (ER), progesterone (PR) and Her2 receptor status and **B)** tumor stage (Note: the "AN, Stage 4" group contains only 2 samples, precluding statistical analyses). Each box plots indicates the sample median and surrounding first and third quartiles. Gene expression processing and statistical analysis are described in *Methods*. Whiskers indicate interquartile range. Asterisks indicate significant differences, *p<0.05, ***p<0.001.

Figure 4. TDO mRNA and protein expression in breast cancer cell lines. A) Cell lines were grown to 70% confluency and analyzed by RT-qPCR for *TDO2* mRNA expression. Gene expression levels were normalized to *18S* RNA levels and the fold-difference relative to the non-malignant mammary epithelial cell line MCF10F was calculated using $\Delta\Delta$Ct values and the Pfaffl method. A low but consistent signal was detected in MCF10F cells at an average of 31 cycles. Data are presented as means + standard errors from 3 experiments. Simple one-way analysis of variance (ANOVA) was used to determine significance.

Molecular Pharmacology Fast Forward. Published on August 29, 2016 as DOI: 10.1124/mol.116.105361
This article has not been copyedited and formatted. The final version may differ from this version.

Asterisks indicate a significant difference relative to *TDO2* expression in MCF10F cells, ****p<0.0001. **B)** A representative western immunoblot (4 experiments total) of TDO and, as a control, β-actin protein expression in mammary epithelial cell lines. Supplemental Figure S6 shows the entire western blot in more detail (see Additional File 6). **C)** Band densities were determined from TDO western immunoblots and normalized to β-actin band densities. Data are presented as means + standard errors from 4 experiments. Data are presented as means + standard errors from 3 experiments. Simple one-way analysis of variance (ANOVA) was used to determine significance. Asterisks indicate a significant increase in β-actin-normalized TDO expression relative to expression in MCF10F cells, ****p<0.0001.

Figure 5. *TDO2* knockdown reduces AHR activity in Hs578T cells. Hs578T cells were stably transduced with scrambled control shRNA or *TDO2*-specific shRNA (**A-C**) or transiently transfected with scrambled or *TDO2*-specific siRNA (**D-F**). Cells were assayed by RT-qPCR for *TDO2* (A, D) or *CYP1B1* (B, E). Gene expression levels were normalized to *18S* RNA and fold-differences were calculated relative to non-transfected cells using the Pfaffl method. Each result is represented as a fold-difference relative to mean of control groups. In “C” and “F”, cells also were transfected with the AHR-driven *pGudLuc* reporter plasmid and, for normalization for transfection efficiency, with *CMV-green* plasmid and assayed 24 hours later for luciferase activity and green fluorescence. Data are presented as the means + standard errors from 4-10 experiments. Student’s T-test was used to determine significance. Asterisks indicate significant decreases in normalized gene expression or pGudLuc activity, *p<0.05, ***p<0.001.

Figure 6. Kynurenine, xanthurenic acid and kynurenic acid induce AHR activity in MCF10F cells. MCF10F cells were transfected with *pGudLuc* and *CMV-green* control reporter plasmids and left untreated or treated with vehicle or 0.1–400 μM kynurenine, xanthurenic acid or kynurenic acid with or without 10 μM of the AHR-specific antagonist, CH223191. The CMV-green-normalized RLU value in each experimental group was normalized to CMV-green-normalized RLU values from untreated cells. Data from 3-5 experiments are presented as means + standard errors. Asterisks indicate significant increases in AHR activity compared to vehicle-treated groups, *p<0.05, **p<0.01, ***p<0.001. Simple one-way analysis of

Molecular Pharmacology Fast Forward. Published on August 29, 2016 as DOI: 10.1124/mol.116.105361
This article has not been copyedited and formatted. The final version may differ from this version.

variance (ANOVA) was used to determine significance. Superscript crosses ($^{+}$) indicate significant decreases in AHR activity following AHR antagonist treatment, as determined by T-test, $^{+}p<0.05$, $^{++}p<0.01$, $^{+++}p<0.0001$.

Figure 7. Tryptophan metabolites in the kynurenine pathway are detected in Hs578T cell lysates. A) Representative chromatograms showing kynurenine (KYN), xanthurenic acid (XA) and kynurenic acid (KA) peaks detected by LC/MS in blanks, positive metabolite controls, and Hs578T lysates. Positive controls (solutions of commercially obtained metabolites) were used to identify peaks in test samples (indicated by arrows). The area under each peak is linearly dependent on metabolite concentration. Titered concentrations of each metabolite were used to create standard curves for calculating sample metabolite concentrations. **B)** Intracellular metabolite concentrations (μM) were determined from sample metabolite concentrations obtained as described in "A", the number of cells used to produce cell lysates, and the approximate mammalian epithelial cell volume of $2{,}000^3$ μm.

Figure 8. TDO-dependent accumulation of kynurenine in Hs578T cell supernatant. A) Hs578T, SUM149 and MDA-MB-231 cells were grown in 6-well plates and fed with 1 ml per well of medium supplemented with vehicle (Hs578T, SUM149 and MDA-MB-231 cells, "O") or enough tryptophan to equal tryptophan concentration in MDA-MB-231 media base (Hs578T and SUM149 cells, "X"). Supernatants were then collected from separate wells at each time point (0, 55, 72 and 92 hours). Collected supernatants were treated with 30% (v/v) trichloroacetic acid and 4-p-dimethylaminobenzaldehyde in glacial acetic acid and assayed for kynurenine accumulation using the colorimetric method described in the *Methods* section. Data shown are means $\pm$ standard errors from 3-9 independent experiments. LC/MS was used to quantify the kynurenine concentration in supernatant at 92 hours (arrow/150 μM). **B)** Hs578T cells were stably transduced with scrambled control shRNA or *TDO2*-specific shRNA and *TDO2* knockdown was confirmed as described in Figure 5A. Supernatants were collected at each time point (0, 24, 55, 76 and 92 hours) and assayed for kynurenine concentration as described in "A". Data are presented as means $\pm$ standard errors from 3 independent experiments. Student's T-test was used to determine significance.

Molecular Pharmacology Fast Forward. Published on August 29, 2016 as DOI: 10.1124/mol.116.105361
This article has not been copyedited and formatted. The final version may differ from this version.

Asterisks indicate a significant reduction in kynurenine relative to levels in cells transfected with control shRNA. *p<0.05, **p<0.01.

Figure 9. TDO over-expression increases kynurenine production, enhances baseline AHR activity, and accelerates migration of SUM149 cells. SUM149 cells were stably transduced with control plasmid or *TDO2* plasmid. TDO over-expression was confirmed via qPCR and Western blot analysis (data not shown). **A)** Control plasmid and *TDO2*-transduced SUM149 cells were plated in 6-well plates, allowed to adhere overnight and fed with 1 ml per well of fresh medium at time 0. Supernatants were collected at time 0 and at 48 hours and assayed for kynurenine production as described in "8A". Data are presented as time 0-normalized absorbance means + standard errors from 4 independent experiments. Student's T-test was used to determine significance. An asterisk indicates a significant increase in kynurenine, p<0.05. **B)** Control plasmid and *TDO2*-transduced SUM149 cells were transfected with the AHR-driven *pGudLuc* reporter plasmid and, for normalization for transfection efficiency, with *CMV-green* plasmid and assayed 48 hours later for luciferase activity and green fluorescence. Data are presented as means + standard errors from 4 independent experiments. Student's T-test was used to determine significance. An asterisk indicates a significant increase in AHR activity, p<0.05. **C)** Confluent layers of control plasmid or *TDO2*-transduced SUM149 cells were scratched and left untreated or treated with vehicle or the AHR antagonist CH223191. Representative photos taken at 48 hours from one of 7 experiments are presented. Black lines indicate borders of the original scratch wound. **D)** For the 7 experiments described in "C", the percent exposed area at 48 hours, relative to the percent exposed area at time 0, was quantified using TScratch™ imaging software. Data are presented as means + standard errors. Student's T-test was used to determine significance. Asterisks indicate significant differences in the time 0 - normalized percent exposed area from the respective control plasmid-transfected groups (no brackets) or between the groups indicated by the brackets , *p<0.05, **p<0.01

Figure 10. Kynurenine and xanthurenic acid accelerate migration of SUM149 cells. Confluent layers of SUM149 cells were scratched and treated with vehicle or the indicated doses of kynurenine (KYN) or xanthurenic acid (XA) or a combination of KYN and XA with or without CH223191. **A)** Representative

photos from one of 5-17 experiments are presented. Black lines indicate borders of the original scratch wound. **B**) For the 5-17 experiments described in "A", the percent exposed area at 36 hours, relative to the exposed area at time 0, was quantified using TScratch™ imaging software. Data are presented as means + standard errors. Data are presented as means + standard errors from 3 experiments. Simple one-way analysis of variance (ANOVA) was used to determine significance. Asterisks indicate a significant decrease in exposed area (i.e., increased migration) compared to vehicle-treated cells or between groups indicated by brackets, **p<0.01, ***p<0.001. Superscript crosses ($^{+}$) indicate a significant increase in exposed area (slowing of migration) after addition of metabolite(s) with 10 μM CH223191, $^{++++}$p<0.0001.

Figure 11. Environmental AHR ligands accelerate migration of SUM149 cells. A) Confluent layers of SUM149 cells were scratched and treated with vehicle, 0.5 μM FICZ, 1 μM B[a]P, or 1 nM TCDD as described in the *Methods* section, and photographed at time 0 and at 36 hours. Black lines indicate the borders of the original scratch wound. Presented are representative images from one of 4 (FICZ) or 5 (B[a]P, TCDD) independent experiments. **B)** For the experiments described in "A", the percent exposed area at 36 hours was quantified using TScratch™ imaging software. Data are presented as the mean exposed area, normalized to time 0 + standard errors. Simple one-way analysis of variance (ANOVA) was used to determine significance. Asterisks indicate a significant decrease in exposed area (i.e., increased migration) compared to vehicle-treated cells, *p<0.05**,** **p<0.01.

Figure 12. AHR regulates *TDO2* expression in Hs578T cells. A) Hs578T cells stably transduced with doxycycline (DOX)-inducible *AHR*-specific shRNA, were cultured with or without 1.5 μg/ml DOX for 5 days and *TDO2* levels quantified by RT-qPCR. *TDO2* expression was normalized to *18S* RNA and the fold difference relative to *TDO2* levels in non-transfected cells was calculated using the Pfaffl method. Each result is represented as a fold-difference relative to mean of control groups. Data from 3 experiments are presented as means + standard errors. Student's T-test was used to determine significance. An asterisk indicates a significant reduction in *TDO2* levels, *p<0.05. **B)** Hs578T cells were treated with vehicle or 10 μM CH223191 for 5 days and *TDO2* expression quantified by RT-qPCR as described in "A". Data from 3

Molecular Pharmacology Fast Forward. Published on August 29, 2016 as DOI: 10.1124/mol.116.105361
This article has not been copyedited and formatted. The final version may differ from this version.

experiments are presented as means + standard error. Student's T-test was used to determine significance. An asterisk indicates significant reduction in *TDO2* levels, *p<0.05. **C)** BP1 cells were stably transduced with doxycycline (DOX)-inducible *AHR*-specific shRNA and cultured and analyzed as described for Hs578T cells in "A". Data from 3 experiments are presented as means + standard errors. Student's T-test was used to determine significance. An asterisk indicates a significant reduction in *TDO2* levels, *p<0.05.

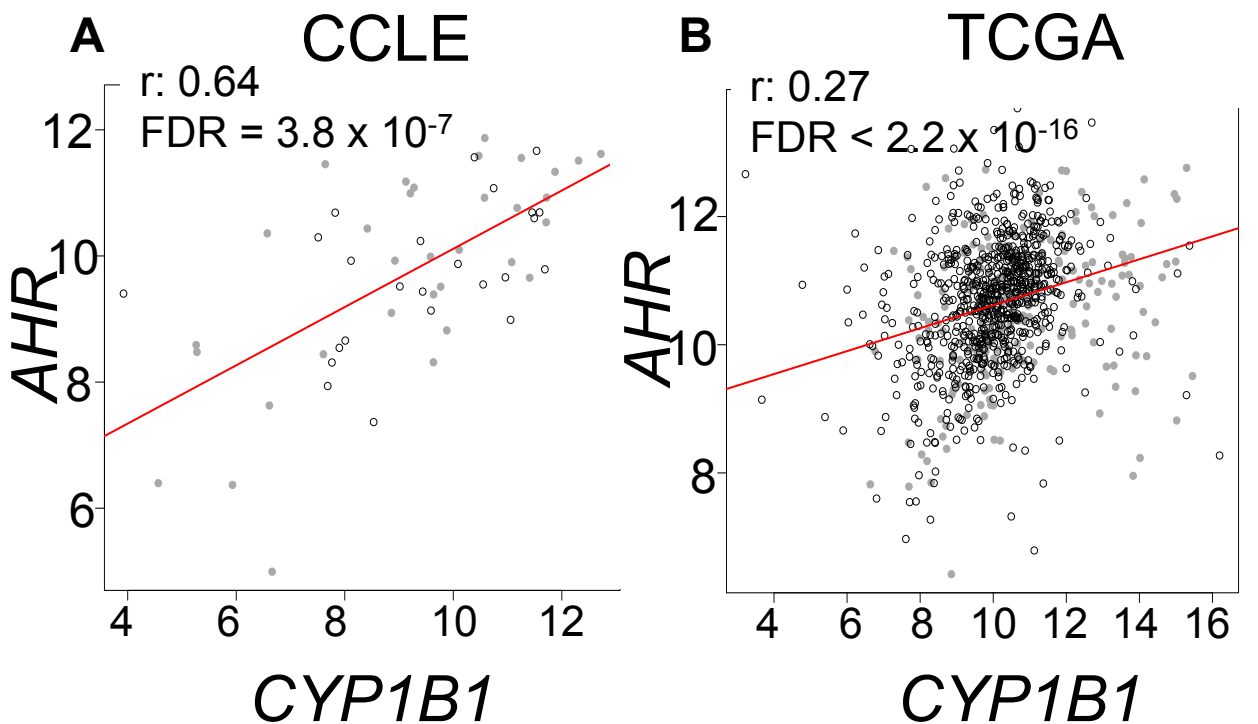
A
CCLE
r: 0.64
FDR = 3.8 x 10-7
AHR
CYP1B1
B
TCGA
r: 0.27
FDR < 2.2 x 10-16
AHR
CYP1B1

Figure 1

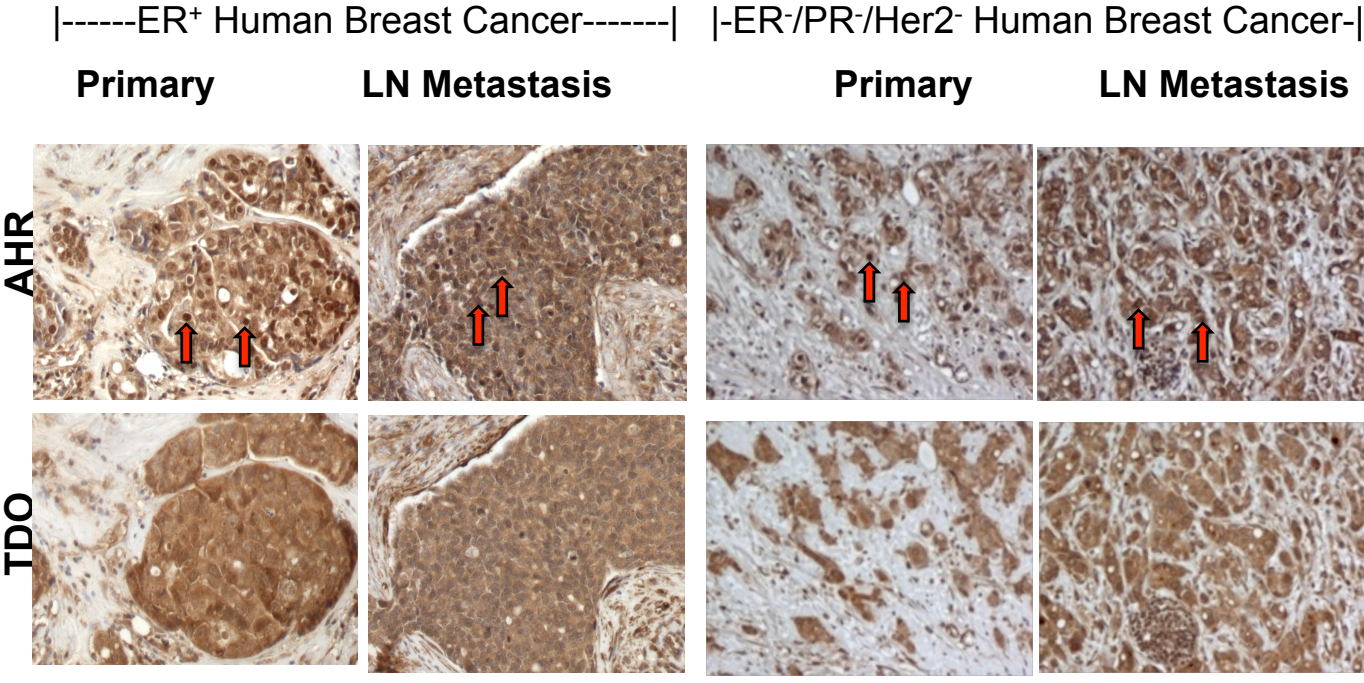
|------ER+ Human Breast Cancer-------|
|-ER-/PR-/Her2- Human Breast Cancer-|
Primary
LN Metastasis
Primary
LN Metastasis
AHR
TDO

Figure 2

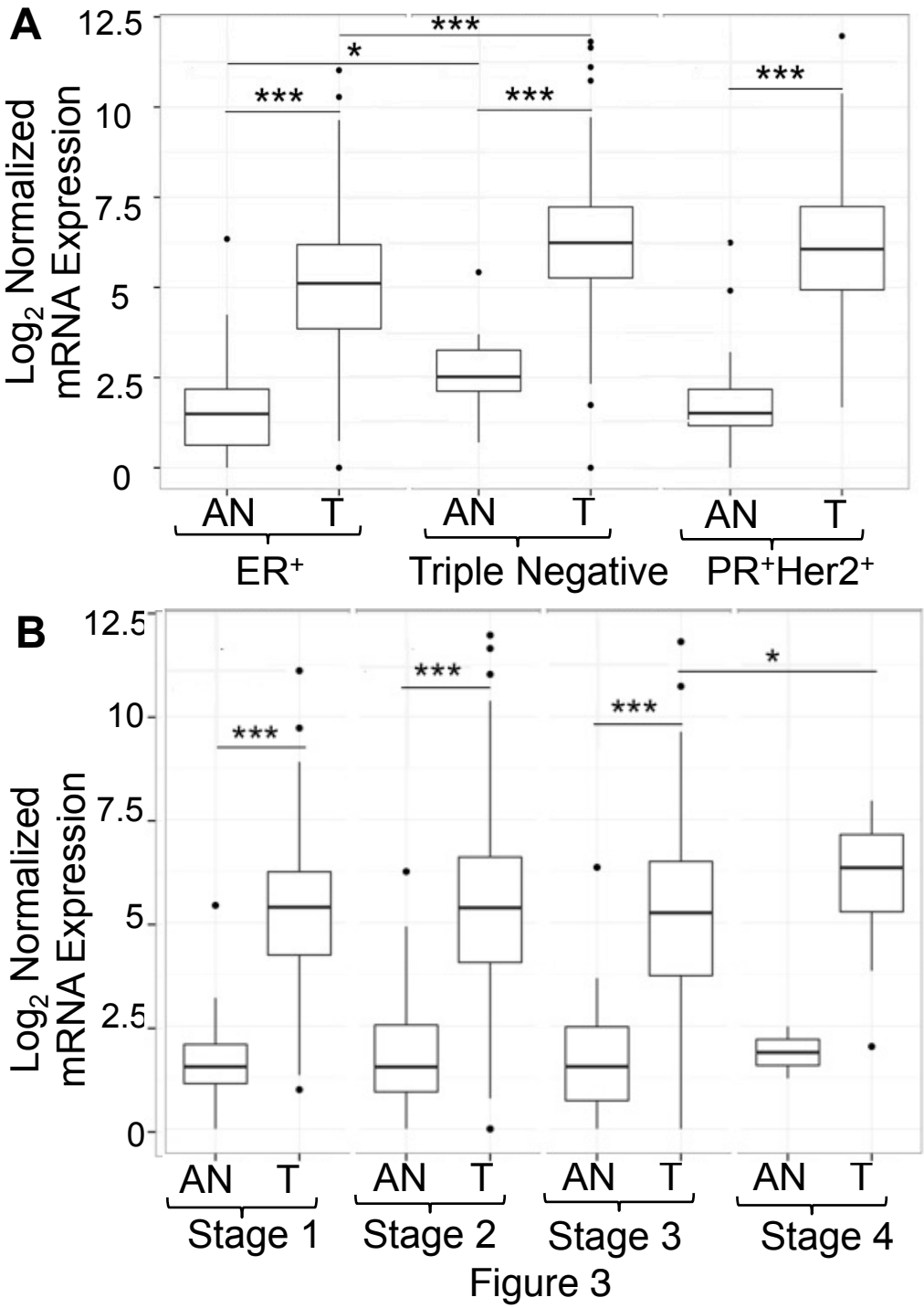
A
Log2 Normalized mRNA Expression
12.5
10
7.5
5
2.5
0
***
*
***
***
***
AN
T
ER+
Triple Negative
PR+Her2+
B
Log2 Normalized mRNA Expression
12.5
10
7.5
5
2.5
0
***
***
***
*
AN
T
Stage 1
Stage 2
Stage 3
Stage 4

Figure 3

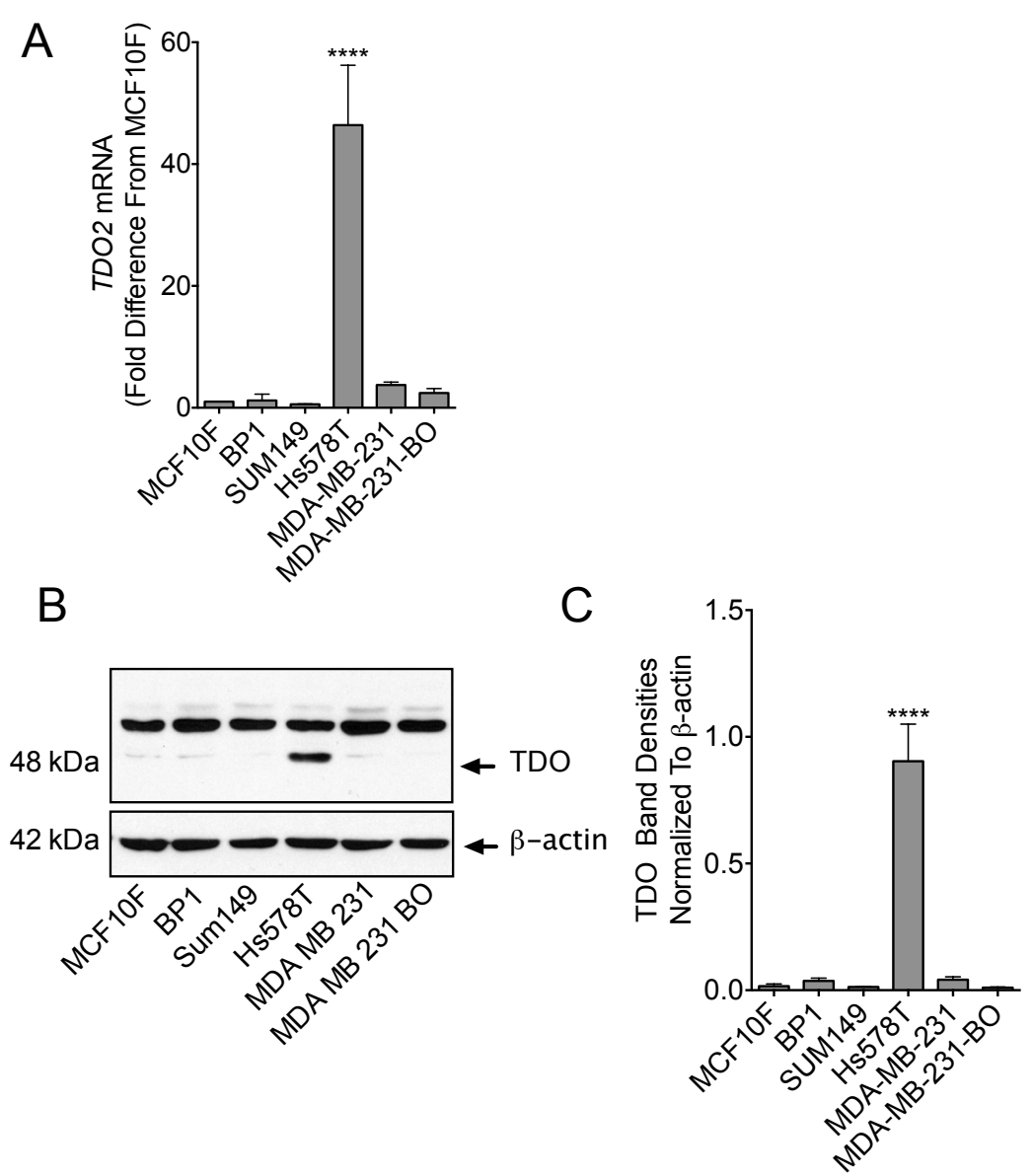
A
TDO2 mRNA
(Fold Difference From MCF10F)
60
40
20
0
****
MCF10F
BP1
SUM149
Hs578T
MDA-MB-231
MDA-MB-231-BO
B
48 kDa
42 kDa
TDO
β-actin
MCF10F
BP1
Sum149
Hs578T
MDA MB 231
MDA MB 231 BO
C
TDO Band Densities
Normalized To β-actin
1.5
1.0
0.5
0.0
****
MCF10F
BP1
SUM149
Hs578T
MDA-MB-231
MDA-MB-231-BO

Figure 4

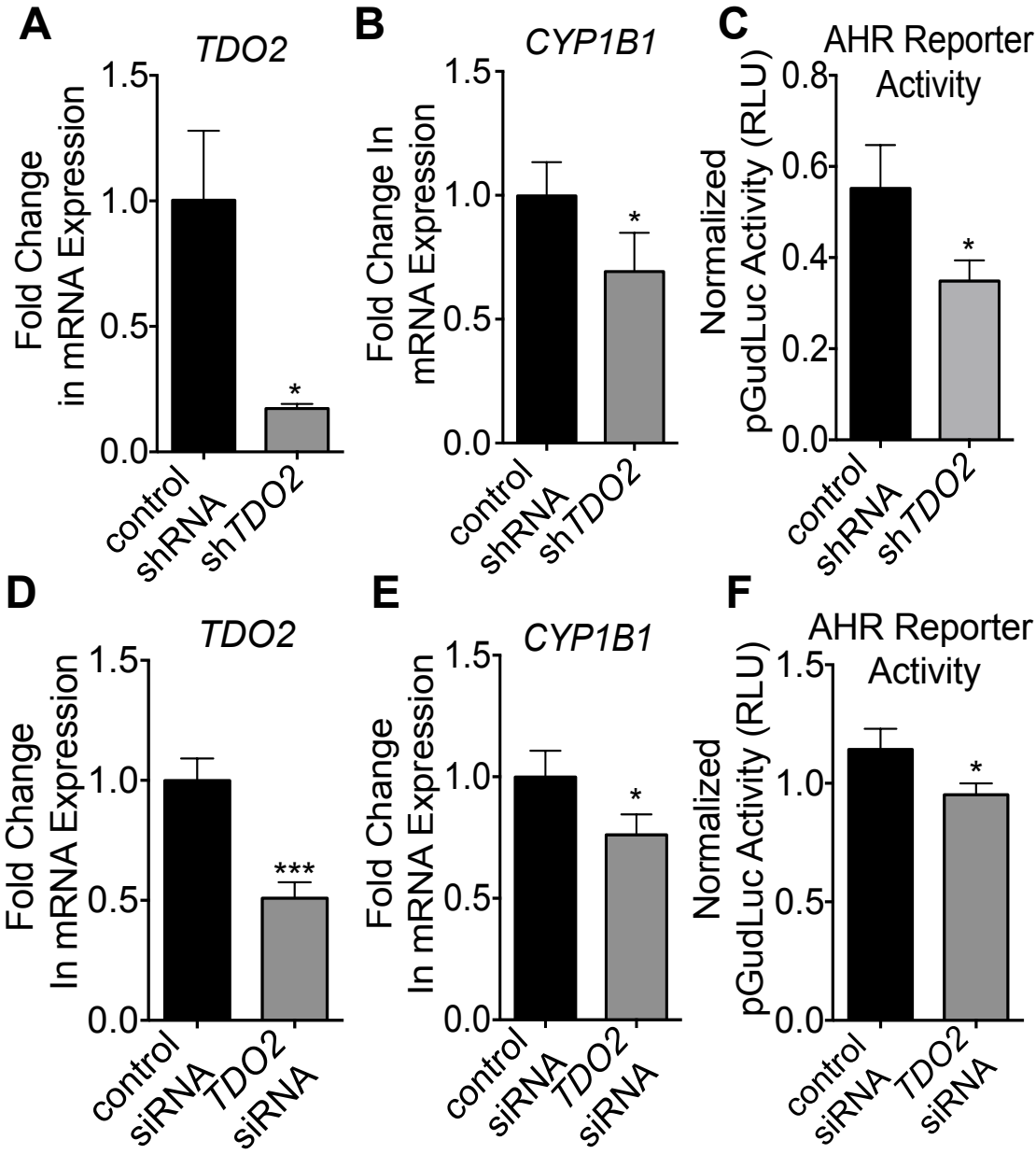
A
TDO2
Fold Change in mRNA Expression
1.5
1.0
0.5
0.0
*
control shRNA
shTDO2
B
CYP1B1
Fold Change In mRNA Expression
1.5
1.0
0.5
0.0
*
control shRNA
shTDO2
C
AHR Reporter Activity
Normalized pGudLuc Activity (RLU)
0.8
0.6
0.4
0.2
0.0
*
control shRNA
shTDO2
D
TDO2
Fold Change In mRNA Expression
1.5
1.0
0.5
0.0
***
control siRNA
TDO2 siRNA
E
CYP1B1
Fold Change In mRNA Expression
1.5
1.0
0.5
0.0
*
control siRNA
TDO2 siRNA
F
AHR Reporter Activity
Normalized pGudLuc Activity (RLU)
1.5
1.0
0.5
0.0
*
control siRNA
TDO2 siRNA

Figure 5

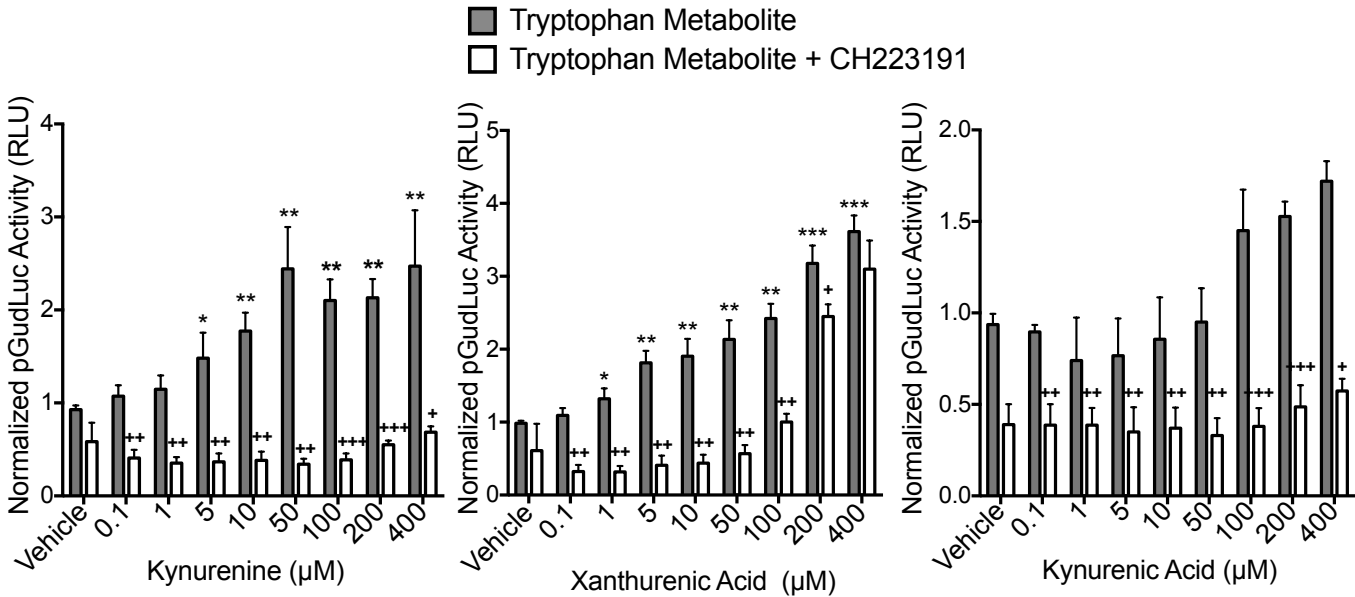
Tryptophan Metabolite
Tryptophan Metabolite + CH223191
Normalized pGudLuc Activity (RLU)
Vehicle
0.1
1
5
10
50
100
200
400
Kynurenine (μM)
Xanthurenic Acid (μM)
Kynurenic Acid (μM)

Figure 6

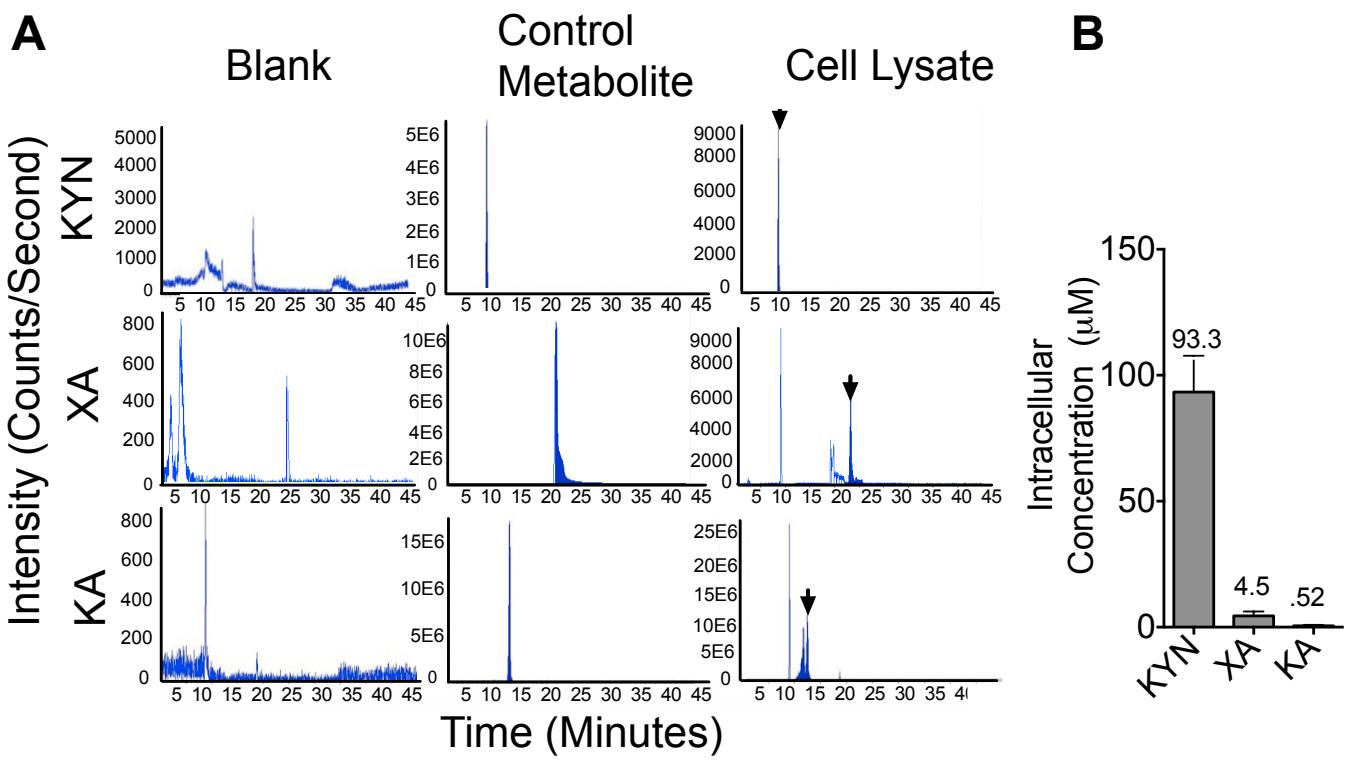
A
Blank
Control Metabolite
Cell Lysate
KYN
XA
KA
Intensity (Counts/Second)
Time (Minutes)
B
Intracellular Concentration (μM)
93.3
4.5
.52
KYN
XA
KA

Figure 7

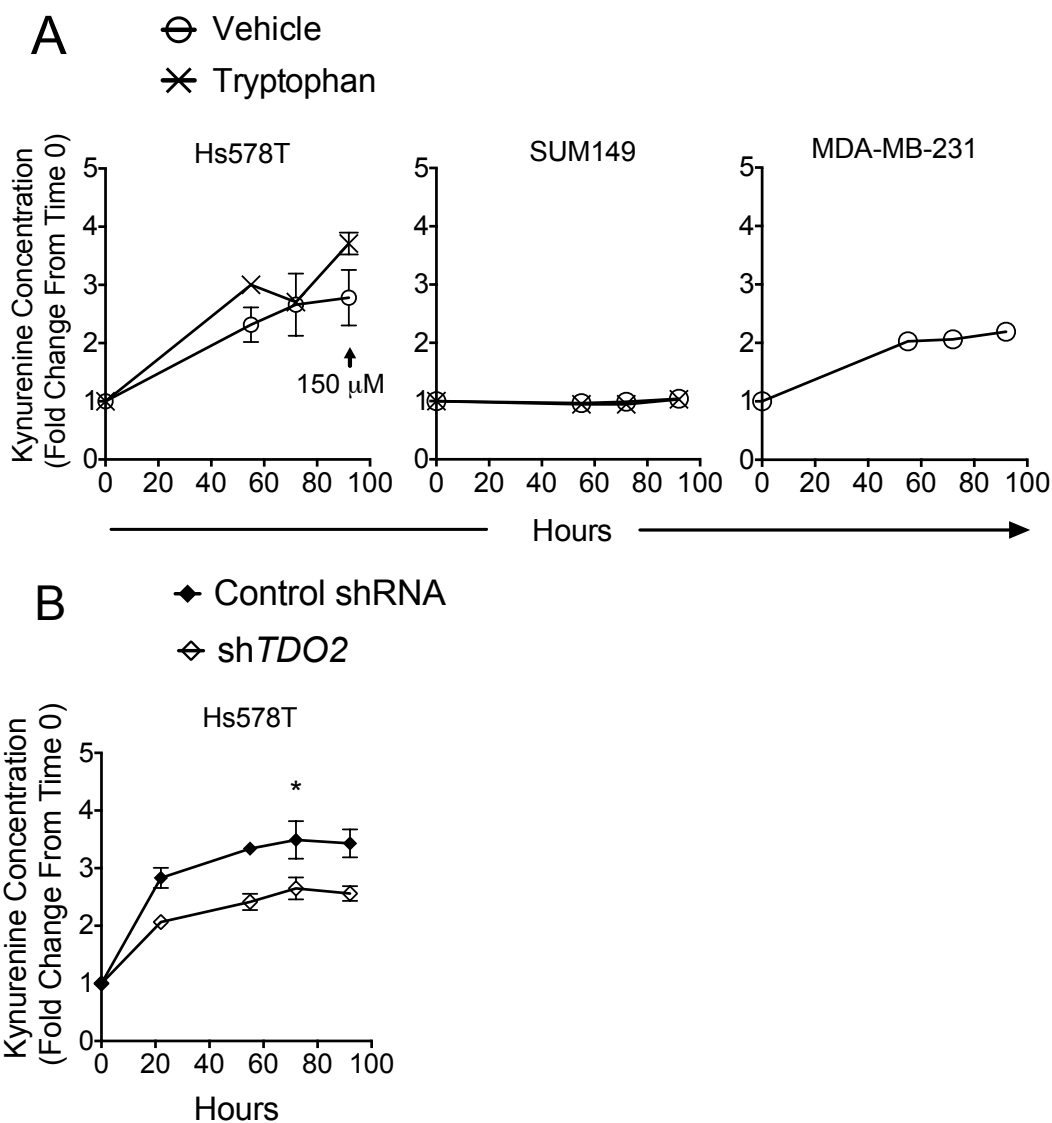
A
Vehicle
Tryptophan
Hs578T
SUM149
MDA-MB-231
Kynurenine Concentration
(Fold Change From Time 0)
150 μM
Hours
B
Control shRNA
sh*TDO2*
Hs578T
Kynurenine Concentration
(Fold Change From Time 0)
*
Hours

Figure 8

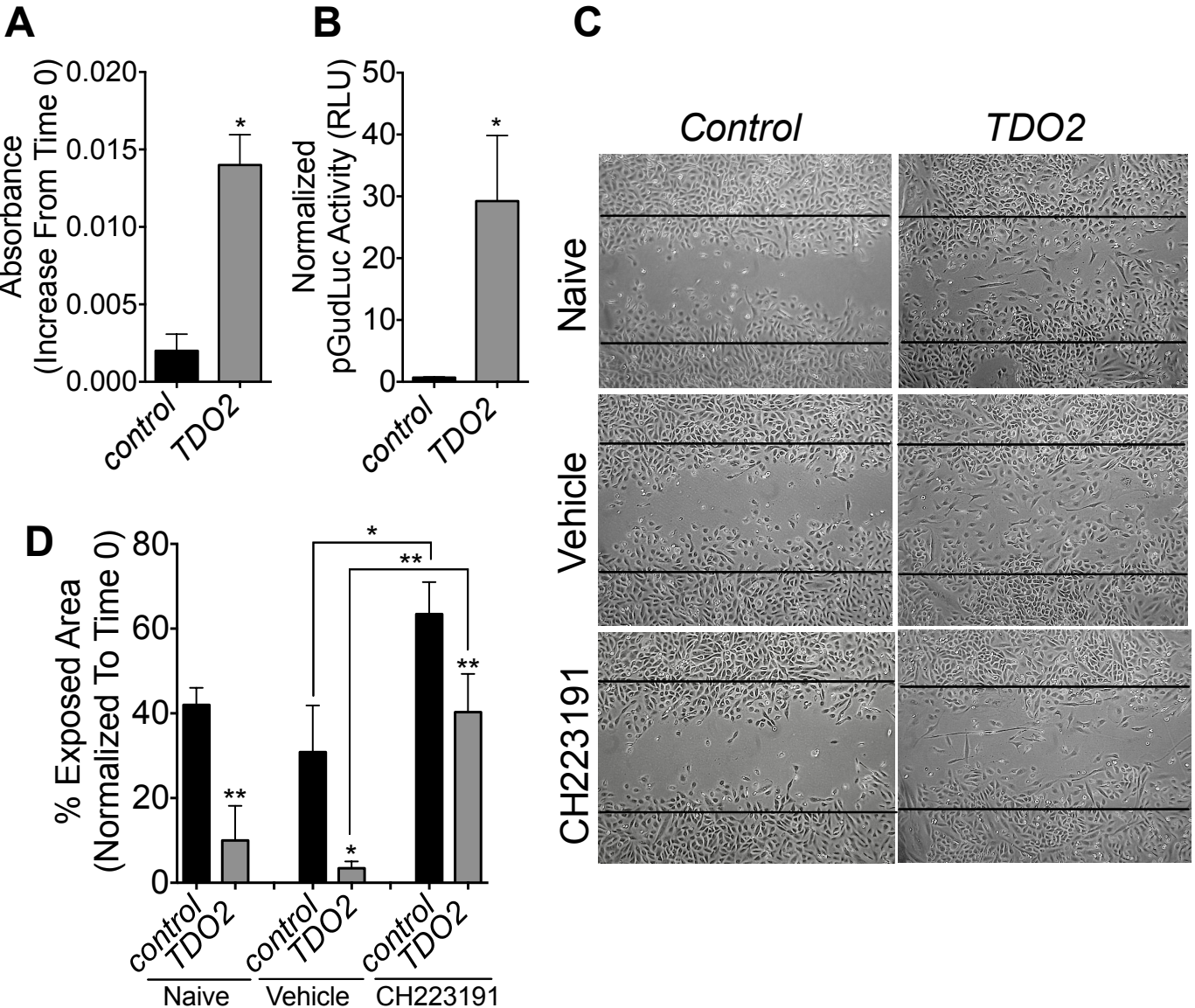
A
Absorbance (Increase From Time 0)
0.020
0.015
0.010
0.005
0.000
*
control
TDO2
B
Normalized pGudLuc Activity (RLU)
50
40
30
20
10
0
*
control
TDO2
C
Control
TDO2
Naive
Vehicle
CH223191
D
% Exposed Area (Normalized To Time 0)
80
60
40
20
0
*
**
**
*
**
control
TDO2
control
TDO2
control
TDO2
Naive
Vehicle
CH223191

Figure 9

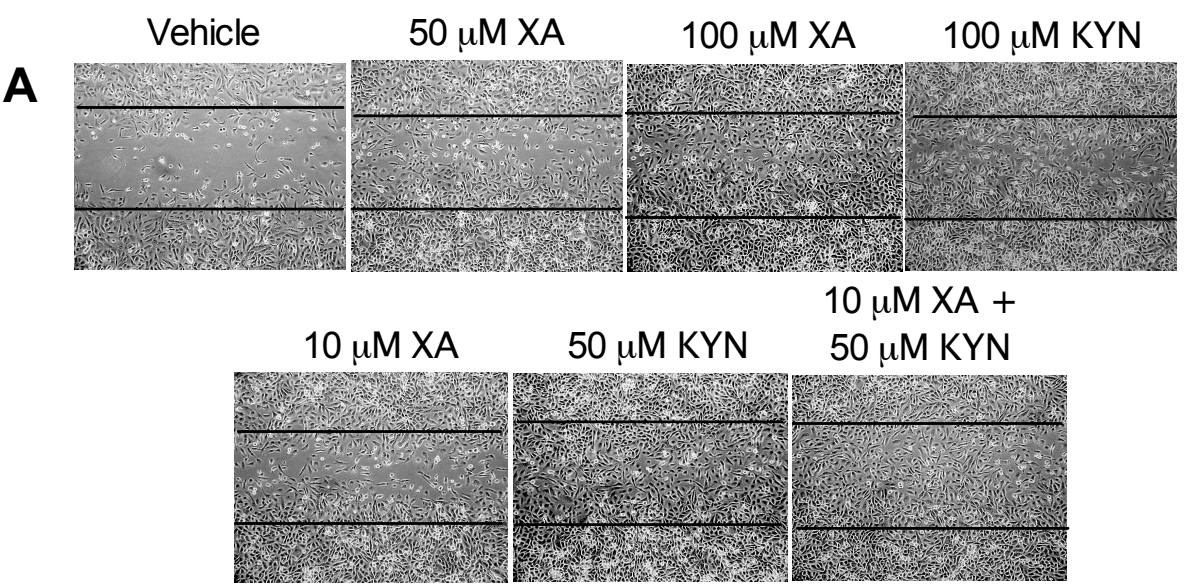
A
Vehicle
50 μM XA
100 μM XA
100 μM KYN
10 μM XA
50 μM KYN
10 μM XA +
50 μM KYN

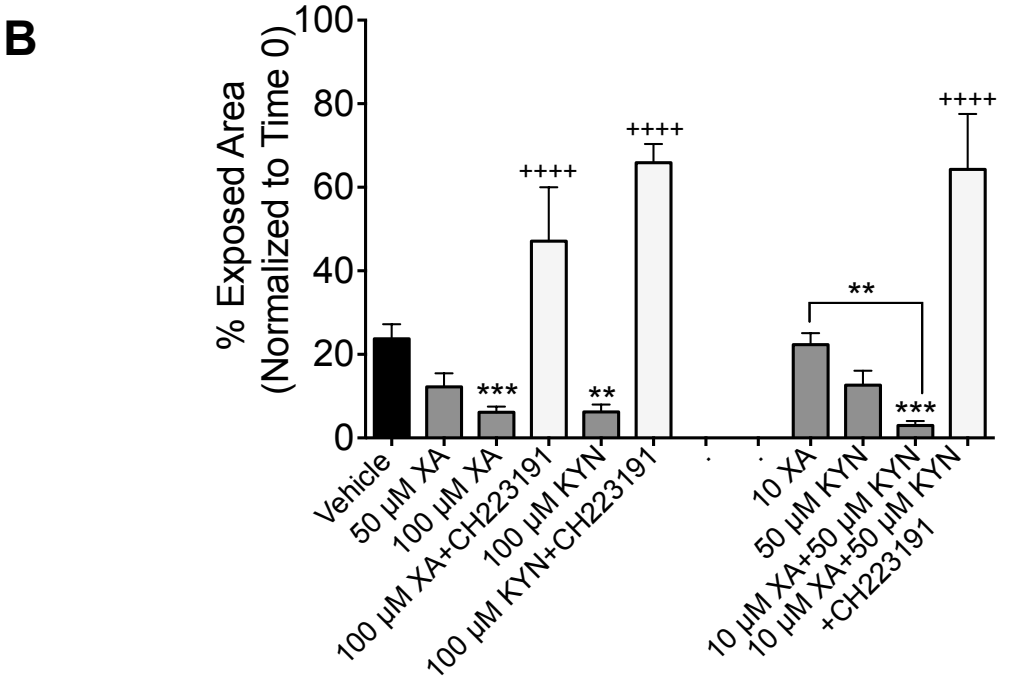
B
% Exposed Area
(Normalized to Time 0)
100
80
60
40
20
0
***
**
++++
++++
**
++++
***
Vehicle
50 μM XA
100 μM XA
100 μM XA+CH223191
100 μM KYN
100 μM KYN+CH223191
10 XA
50 μM KYN
10 μM XA+50 μM KYN
10 μM XA+50 μM KYN
+CH223191

Figure 10

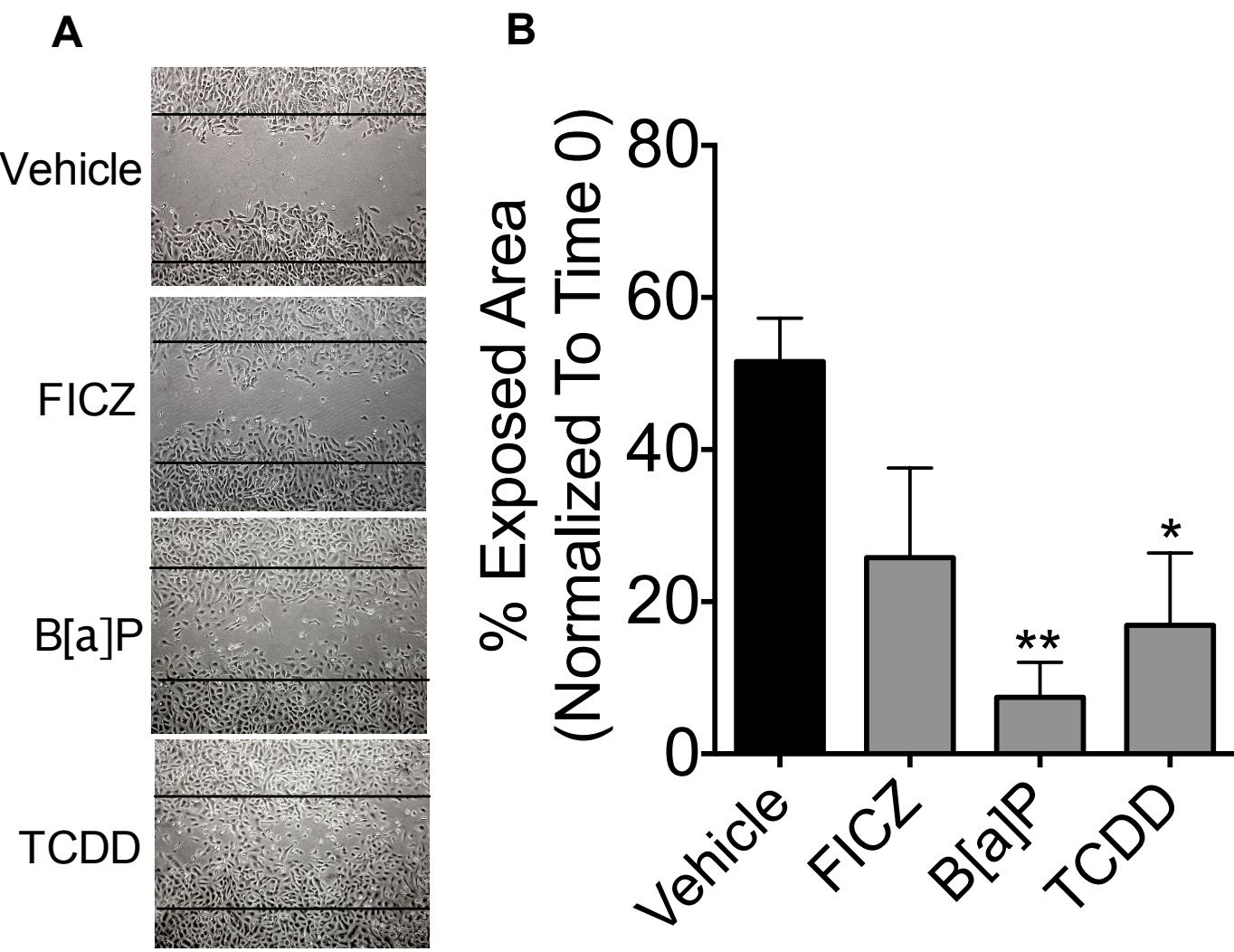
A
Vehicle
FICZ
B[a]P
TCDD
B
% Exposed Area
(Normalized To Time 0)
80
60
40
20
0
**
*
Vehicle
FICZ
B[a]P
TCDD

Figure 11

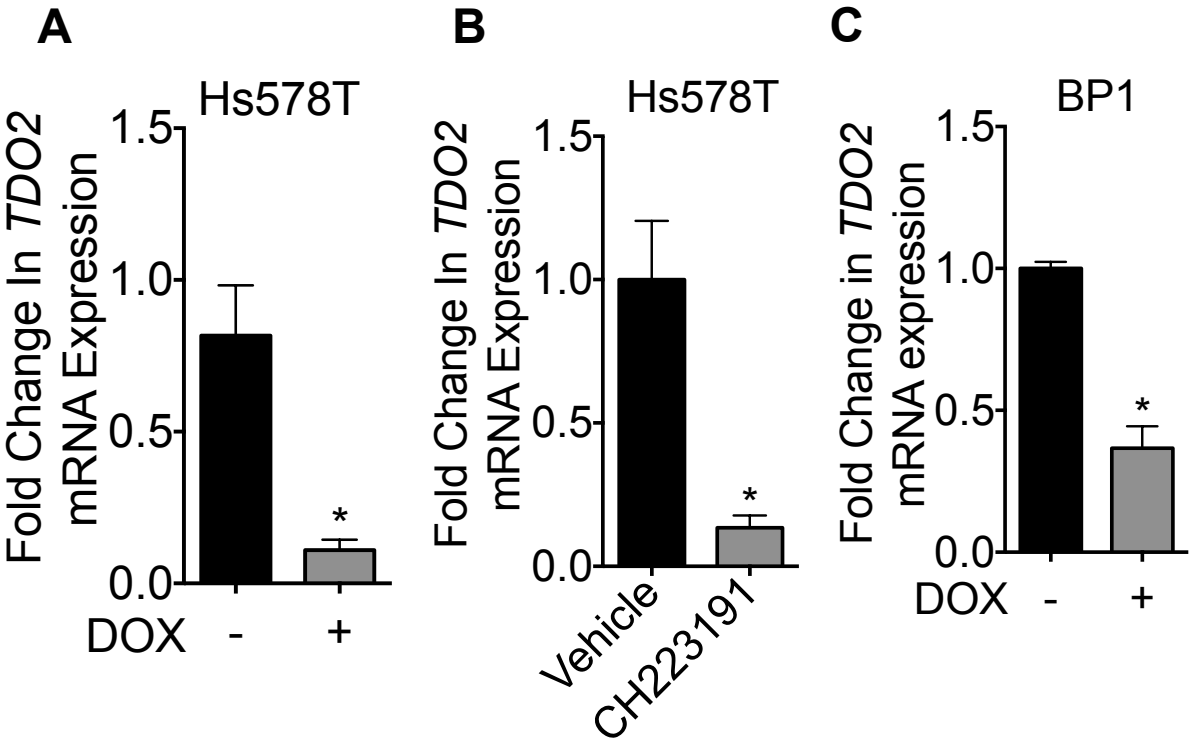
A
Hs578T
Fold Change In TDO2 mRNA Expression
1.5
1.0
0.5
0.0
*
DOX - +
B
Hs578T
Fold Change In TDO2 mRNA Expression
1.5
1.0
0.5
0.0
*
Vehicle
CH223191
C
BP1
Fold Change in TDO2 mRNA expression
1.5
1.0
0.5
0.0
*
DOX - +

Figure 12